iScience

Article

Single cell profiling of hematopoietic stem cell transplant recipients reveals TGF-β1 and IL-2 confer immunoregulatory functions to NK cells

Graphical abstract

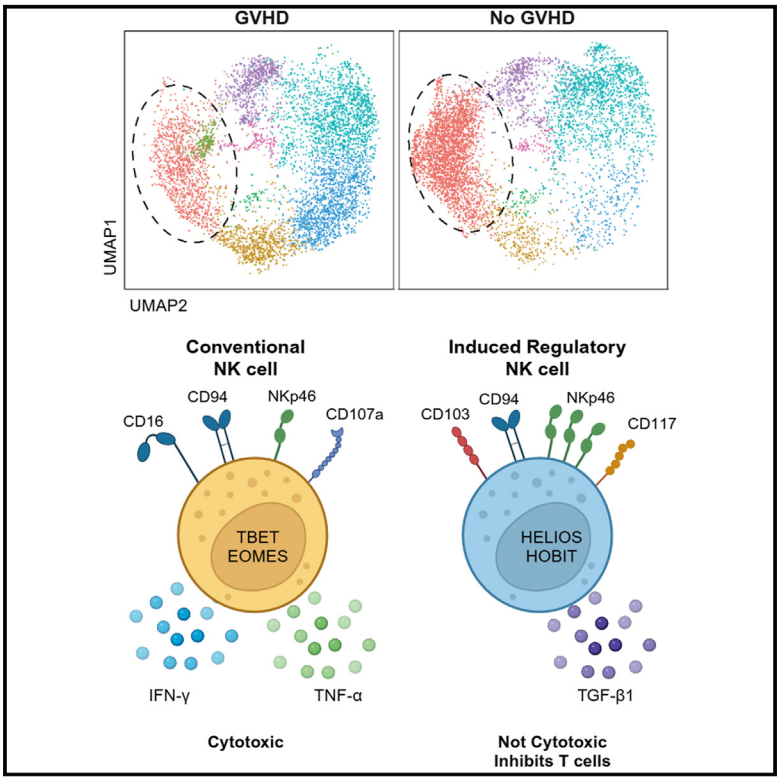

Highlights

- scRNA-seq identifies a *TGFβ1*^{high}*CD56*^{bright}NK cell population in HSCT patients without GVHD
- IL-2 and TGF-β1 induce similar transcriptional programs in NK cells from normal donors
- IL-2 and TGF-β1-induced immunoregulatory NK cells secrete TGF-β1 and suppress T cells
- These "induced" regulatory NK cells are not a stable cell state

Authors

Jessica A. Mathews, Dorota T. Borovsky, Kyle T. Reid, ..., Jonas Mattsson, Pamela S. Ohashi, Sarah Q. Crome

Correspondence

sarah.crome@utoronto.ca

In brief

NK cells exhibit diverse functions shaped by cytokines and microenvironments. We identify TGF-β1^{high}CD56bright NK cells linked to protection from GVHT post-HSCT. IL-2 and TGF-β1 drive NK cells to a transient regulatory phenotype with unique transcriptional profiles, highlighting non-canonical regulatory functions can be induced by these cytokines.

Mathews et al., 2024, iScience *27*, 111416
December 20, 2024
https://doi.org/10.1016/j.isci.2024.111416

CellPress

iScience

CellPress
OPEN ACCESS

Article

Single cell profiling of hematopoietic stem cell transplant recipients reveals TGF-β1 and IL-2 confer immunoregulatory functions to NK cells

Jessica A. Mathews,[1] Dorota T. Borovsky,[1,2,4] Kyle T. Reid,[1,2,4] Julia M. Murphy,[1,2,4] Sarah J. Colpitts,[1,2] Abel Santos Carreira,[3] Tommy Alfaro Moya,[3] Douglas C. Chung,[2,3] Igor Novitzky-Basso,[3] Jonas Mattsson,[3] Pamela S. Ohashi,[2,3] and Sarah Q. Crome[1,2,5,*]

[1]Toronto General Hospital Research Institute, Ajmera Transplant Centre, University Health Network, Toronto, ON M5G 1L7, Canada
[2]Department of Immunology, Temerty Faculty of Medicine, University of Toronto, Toronto, ON M5S 1A8, Canada
[3]Princess Margaret Cancer Centre, University Health Network, Toronto, ON M5G2C4, Canada
[4]These authors contributed equally
[5]Lead contact
*Correspondence: sarah.crome@utoronto.ca
https://doi.org/10.1016/j.isci.2024.111416

SUMMARY

Natural killer (NK) cell activity is influenced by cytokines and microenvironment factors, resulting in remarkably diverse functions, by contributing to inflammatory responses or serving as rheostats of adaptive immunity. Using single cell RNA sequencing (scRNA-seq), we identified a *TGFβ1*^{high}CD56^{bright}NK cell population associated with hematopoietic stem cell transplant recipients protected from acute graft-versus-host disease (GVHD). We further define a role for the combination of interleukin-2 (IL-2) and transforming growth factor β1 (TGF-β1) in promoting a regulatory phenotype in NK cells. "Induced" regulatory NK cells produce high amounts of TGF-β1, inhibited T cells, could promote naive T cells differentiation into regulatory T cells, and exhibited a unique transcriptional program that includes expression of *IKZF2* (HELIOS) and *ZNF683* (HOBIT). This phenotype was not stable, and "induced" regulatory NK cells lost the ability to secrete TGF-β1 upon exposure to different cytokines. These findings define protective CD56^{bright}NK cells post-hematopoietic stem cell transplantation, and demonstrate the combination of IL-2 and TGF-β1 promotes regulatory activity in NK cells.

INTRODUCTION

Natural killer (NK) cells have essential functions in immune homeostasis, and depending on the context, can either contribute to inflammatory immune responses or instead act as regulators of adaptive immunity.[1,2] Comprising 5%–20% of circulating lymphocytes, NK cells are generally classified as CD56^{bright}CD16^{-} NK cells or CD56^{dim}CD16^{+} NK cells.[3–5] Circulating CD56^{bright} NK cells are described as being more immature, with the capacity to develop into CD56^{dim} NK cells. They have also been described as "regulatory" NK cells, due to their ability to secrete high amounts of interferon (IFN)-γ, tumor necrosis factor alpha (TNF-α), granulocyte macrophage colony stimulating-factor (GM-CSF), and displaying little to no cytotoxicity.[6] In contrast, CD56^{dim} NK cells, which comprise 90%–95% of NK cells in blood, are mature NK cells, express high amounts of cytotoxic molecules and exhibit antibody-dependent cellular cytotoxicity (ADCC) functions via the Fc receptor CD16.[7–9] While these classifications have been used to characterize NK cells historically, it is now understood that NK cells exhibit extensive heterogeneity and can develop diverse memory and tissue-adapted phenotypes.[5,10,11]

Hematopoietic stem cell transplant (HSCT) is often a curative therapy for hematological malignancies. The success of this therapy is mediated in part by donor-derived T cells and NK cells attacking leukemic cells, known as the graft-versus-leukemic (GVL) effect. After HSCT, a high number of circulating NK cells correlates with decreased relapse incidence and lower rates of infection.[12,13] Circulating NK cells in HSCT recipients that contribute to GVL effects are associated with high expression of degranulation marker CD107a by NK cells (<20%).[14] In addition to being associated with beneficial GVL responses, NK cells are also associated with protection from acute graft-versus-host disease (aGVHD), which occurs when donor-derived T cells attack healthy recipient tissues including the gut, skin, liver, and lung. aGVHD affects 30%–60% of HSCT recipients and has a 1-year mortality rates of 35% despite prophylactic cyclophosphamide.[15–18] Recent studies support that specifically CD56^{bright} NK cells are associated with protection from GVHD; HSCT recipients protected from aGVHD have elevated proportions of circulating CD56^{bright} NK cells in comparison to those who developed aGVHD, and a high ratio of NK cells to CD8^{+} T cells is correlated with protection from aGVHD.[13,19–23] Interestingly, the presence of "regulatory" CD56^{bright} NK cells has been

reported in chronic GVHD, characterized as NKp46^{+}granzyme K^{+}CD16^{-} NK cells, with decreased expression of granzyme B and perforin.[24] Further, loss of these regulatory CD56^{bright} NK cells and an increase in naive T cells is associated with onset of chronic GVHD.[25] While there is widespread appreciation of protective functions of NK cells in HSCT, we currently lack detailed understanding of factors that influence post-HSCT NK cell development, phenotypes and activity, particularly in humans.

The function of NK cells is greatly influenced by cytokines within local microenvironments. Activation of human NK cells via interleukin (IL)-15, IL-18, and IL-12 results in acquisition of memory-like properties with increased activity toward acute myeloid leukemia (AML) cells.[11] In contrast, in the presence of solely IL-2 and IL-12, NK cells were reported to express IL-10 and suppress antigen specific T cells.[26] Cytokines can greatly influence NK cell anti-tumor responses, and can induce non-typical NK cell phenotypes or even NK cell conversion to other innate lymphoid cell (ILC) family members.[27–31] For example, mouse tumor-infiltrating NK cells lose CD49b and EOMES expression and convert into non-cytotoxic ILC1s, when exposed to the immunosuppressive cytokine transforming growth factor β (TGF-β).[32,33] In humans, we described a population of regulatory NK cell-like ILCs in high grade serous ovarian cancer that exhibited distinct functions from conventional NK cells, including the ability to directly inhibit tumor-associated CD4^{+} and CD8^{+} T cells via non-cytotoxic mechanisms.[34] Importantly, these "regulatory" NK cell-like ILCs were associated with early cancer recurrence.[34] While regulatory NK cell-like ILCs in high grade serous ovarian cancer shared many characteristics with NK cells, including an expression of CD94, KIRs, and NKp46, they exhibited a distinct transcription profile, did not produce IFN-γ or TNF-α, and instead expressed cytokines associated with other ILC family members.[34] Several other groups have also reported distinct NK cell populations with immunosuppressive functions in cancer. For example, NKp46^{+}CD56^{dim}CD16^{+} NK cell in non-small cell lung carcinoma tumors correlated with worse overall survival and suppressed tumor-specific IFN-γ secretion from T cells,[29] and a CD73^{+} NK cell population was observed in sarcoma and breast cancer patients that was characterized by the ability to secrete IL-10 and TGF-β1 and inhibited IFN-γ production from CD4^{+} T helper (Th) 1 cells.[27] Further, NK cells with regulatory activity in acute lymphoblastic leukemia patients were identified as a CRTAM^{+} CD56^{+} population with low cytotoxic potential and expression of IL-10 and TGF-β1.[30] Despite these many reports of NK cells with altered functions or acquisition of immunoregulatory functions, the signals that promote regulatory functions by NK cells is not well understood.

In this study, we identified a unique circulating NK cell population in HSCT recipients protected from aGVHD using single-cell RNA sequencing (scRNA-seq). This CD56^{bright} NK cell population was defined by expression of *TGFβ1* and was the predominant NK cell population in HSCT recipients protected from aGVHD, but was only present in very low abundance in HSCT recipients with aGVHD, and was completely absent in healthy donors. Analysis of cytokine receptor expression by this *TGFβ1*$^{+}$ NK cell population revealed high expression of *TGFBR1-3* and *IL2* receptor subunits (β, γ, α subunits). Based on these observations, we explored TGF-β1 and IL-2 effects on human NK cells, and demonstrate that the combination of TGF-β1 and IL-2 promotes acquisition of regulatory functions in CD56^{bright}NK cells. Altogether, our results characterize the synergistic effects of IL-2 and TGF-β1 on NK cells, and define a distinct TGFβ1^{+}NK cell population in HSCT recipients protected from GVHD.

RESULTS

Identification of a TGF-β1^{+}CD56^{bright} NK cell population in HSCT recipients protected from GVHD

To delineate specific features of NK cells in HSCT recipients protected from aGVHD and identify factors that might contribute to their development or activity, circulating NK cells from HSCT recipients that developed grade 3–4 aGVHD (n = 7), or HSCT recipients that did not develop aGVHD (n = 6) were assessed by scRNA-seq (Figure 1A; Table S1). All patients in this cohort received post-transplant prophylactic cyclophosphamide (see Table S1), with 4 of the 7 individuals that developed GVHD receiving additional treatments for 24 h or less, prior to sampling. scRNA-seq was used to enable assessment of heterogeneity of NK cell populations across individuals, to ensure other ILC family members were not included in analysis, and to enable identification of unique features of NK cell post-HSCTs in an unbiased manner. We further compared the phenotype of NK cells following HSCT to circulating NK cells in peripheral blood of healthy donors (n = 8) to determine unique NK cell states in HSCT recipients with differing clinical outcomes.[35] A total of 15,993 NK cells were captured with approximately equal proportions of total NK cells coming from HSCT patients with GVHD (36.4%), without GVHD (36.7%), and healthy donors (26.9%).

Based on *NCAM1* and *FCGR3A* expression, we identified four clusters of CD56^{bright} NK cells and four clusters of CD56^{dim} NK cells (Figure 1A). There were no significant differences in the median proportion of CD56^{dim} NK cells from cluster 1 and cluster 2 between HSCT recipients with and without GVHD, though both patient groups had reduced proportions compared to healthy individuals (Figures 1B and S1A). In contrast, there was an increased median proportion of CD56^{dim} NK cells from cluster 3 in patients with aGVHD and no differences in CD56^{dim} NK cells from cluster 4 (Figures 1B and S1A) Within the CD56^{dim} NK cells, differential gene expression analysis indicated that CD56^{dim} cluster 1 and cluster 2 highly expressed *NKG7*, *FCGR3A*, cytotoxic granules (*GZMK* and *GZMH*) and chemokines (*CCL3*, *CCL4*, and *CCL5*) (Figure 1C). Between these two clusters, CD56^{dim} cluster 1 more highly expressed *PRF1*, *CD81*, *KLRB1*, and chemokine receptors (*CX3CR1* and *CXCR4*) (Figure 1C). While still expressing genes indicative of a CD56^{dim} NK cell, cluster 3 had a unique gene expression profile consisting of *CTSD*, *SEPTIN7*, *SEPTIN9*, and *TLE5* as well as *AREG*, potentially indicating a role in epithelial cell repair, while cluster 4 had was defined by expression of *ITGB1*, a marker of homing, as well as *RORA* typically associated with ILC2s and ILC3s (Figure 1C).

Within the four CD56^{bright} NK cell clusters, cluster 3 was observed to have an increase in median frequency in HSCT recipients with aGVHD, CD56^{bright} cluster 2 has relative equal frequencies across HSCT recipients with aGVHD and healthy

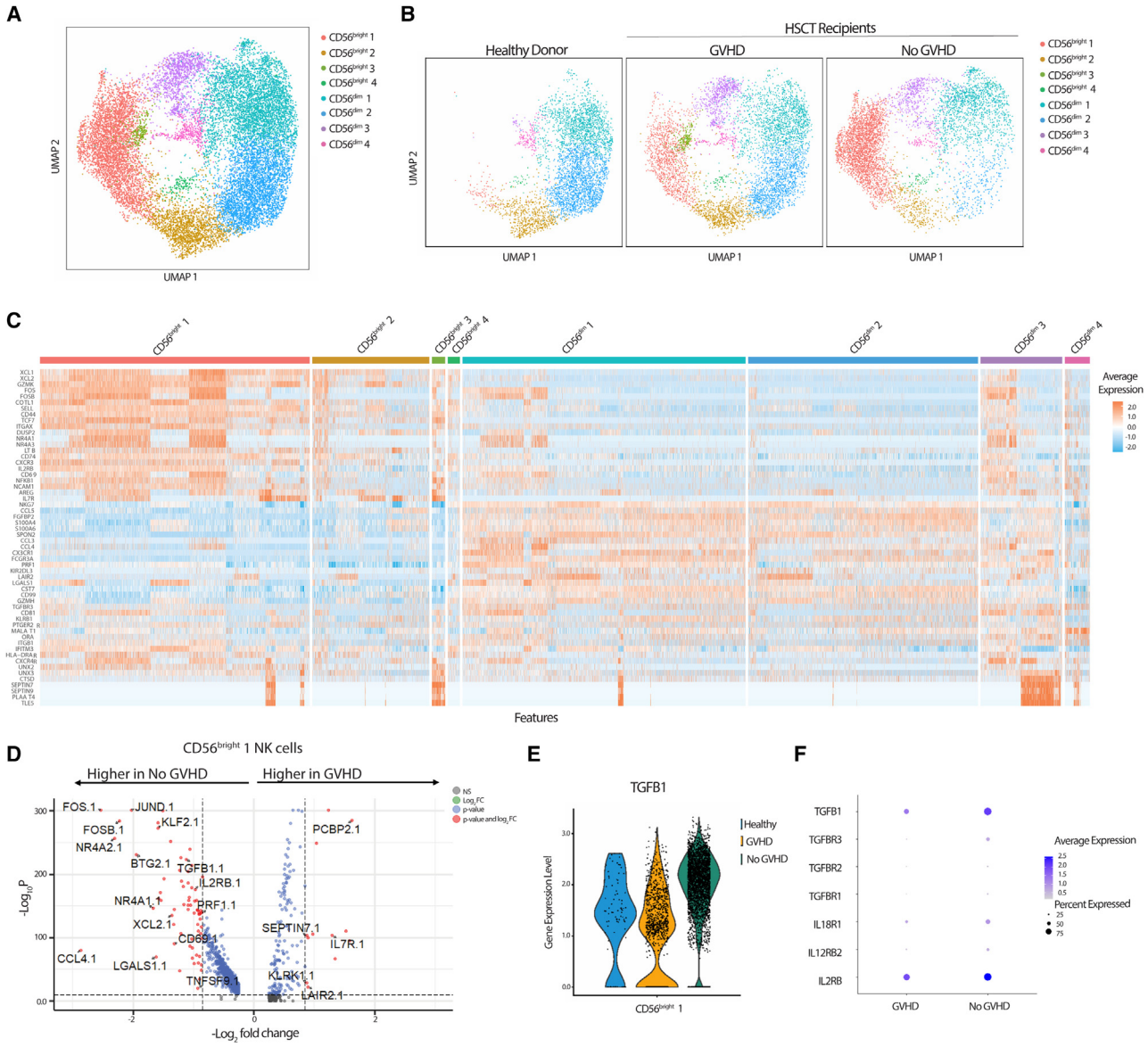

Figure 1. Unique *TGFβ1*$^{+}$CD56^{bright} NK cell population in HSCT recipients protected from GVHD

(A) UMAP clustering of NK cells captured by sequencing PBMCs from healthy (n = 8), HSCT recipients with GVHD (n = 7) and HSCT recipients without GVHD (n = 6).

(B) UMAP plot of NK cells separated by HSCT patients with GVHD, healthy PBMCs and HSCT patients with no GVHD patients.

(C) Heatmap showing differential gene expression between clusters.

(D) Volcano plot showing differential expression of genes between CD56^{bright} NK cells in cluster 1 in patients without GVHD compared to GVHD.

(E) Violin plot of *TGFB1* expression in CD56^{bright} NK cluster 1.

(F) Dot plot representation of cytokine receptors significantly differentially expressed by CD56^{bright} NK cell cluster 1 from HSCT recipients protected from GVHD compared to patients who developed GVHD. Significance was calculated using Wilcoxon rank-sum test and determined to be significant if p value less than 1×10^{-10}.

donors, and CD56^{bright} cluster 1 was significantly elevated in proportion from patients without aGVHD and was virtually absent in healthy controls (Figures 1B and S1A). This cluster comprised a median of 51.96% of all NK cells in the blood of HSCT recipients that did not develop GVHD, supporting that this unique NK cell population is associated with protection from GVHD. The differential gene expression of CD56^{bright} NK cells revealed increased expression of genes associated with tissue homing (*SELL* and *ITGAX*), nuclear receptor family members (*NR4A1* and *NR4A3*) and *GZMK*, while cluster 2 highly expressed chemokines *CCL5* and *IL7R* (Figure 1C). Cluster 3 predominately originating from HSCT recipients with aGVHD had high expression of *IL7R*, *AREG*, and *TCF7*, while also sharing the unique signature seen in CD56^{dim} cluster 3 (Figure 1C). Finally, cluster

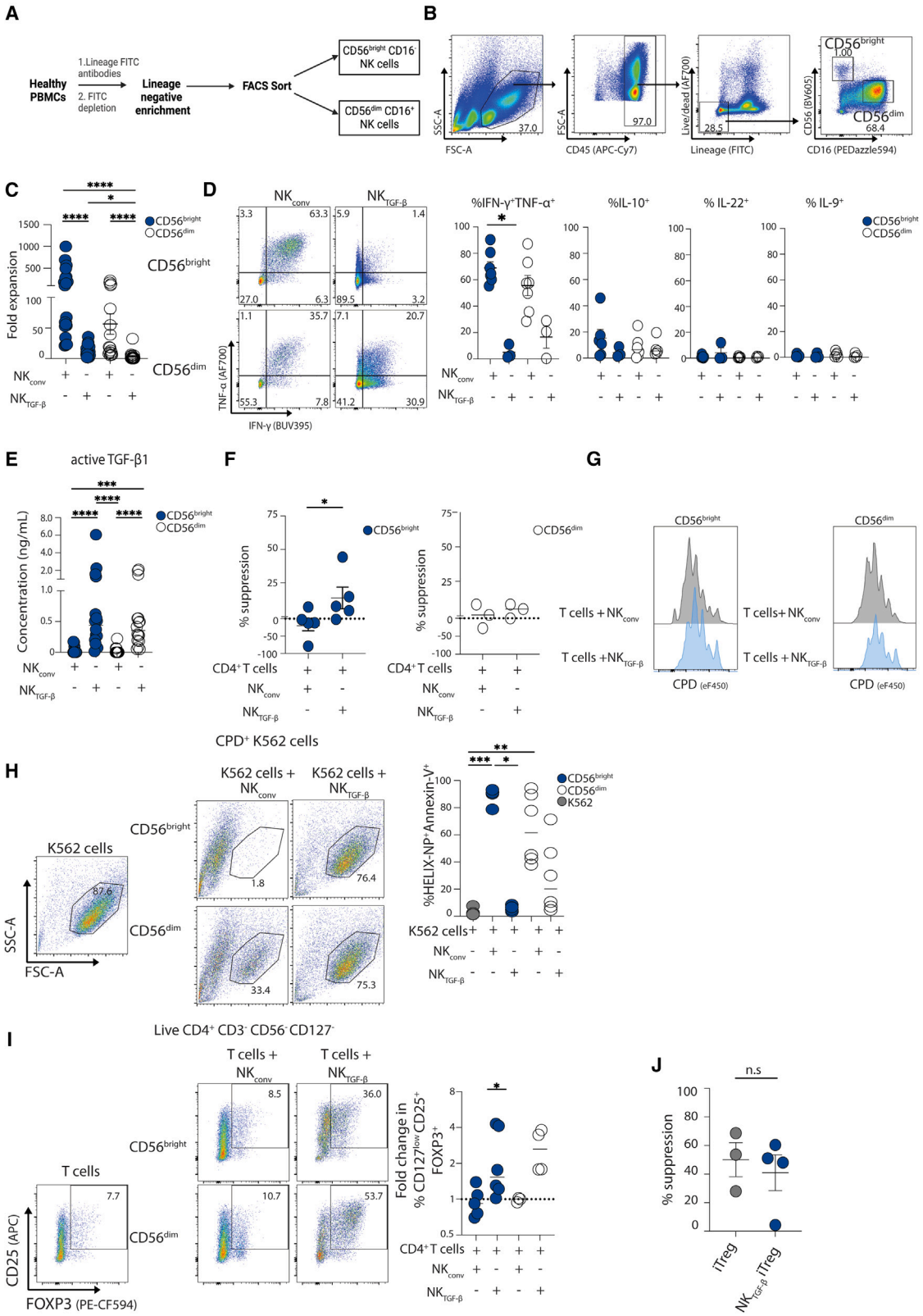

(legend on next page)

4 had elevated expression of *IFITM3*, *ITGB1*, and *HLA-DRA* (Figure 1C).

Based on the significantly increased prevalence of CD56^{bright} cluster 1 in patients without GVHD, we further examined the gene expression profile of this NK cell population. CD56^{bright} cluster 1 had higher expression of transcription factors (*FOS*, *FOSB*, and *TCF7*), chemokines (*XCL1* and *XCL2*), and activation markers (*CD69*) (Figure 1C). We noted CD56^{bright} cluster 1 expressed some molecules previously been reported on regulatory NK cells in the context of chronic GVHD. This included elevated expression of *GZMK*, *IL7R*, *GPR183*, *TNFRSF11A*, *TCF7*, *SELL*, and *XCL1* with decreased expression of *FCGR3A* and *CCL4* compared to other NK cell clusters.[24] Interestingly, the immunosuppressive cytokine *TGFβ1* was highly expressed in CD56^{bright} cluster 1 in patients that did not develop GVHD (Figures 1D and 1E). To confirm TGF-β1 expression was a unique feature of CD56^{bright} NK cells in HSCT recipients that did not have GVHD, CD56^{bright} NK cells from HSCT recipients with and without GVHD were isolated by flow cytometry and assessed for expression of active TGF-β1. TGF-β1 expression was detected in supernatants from sorted CD56^{bright} NK cells from HSCT recipients protected from GVHD following 24-h culture in IL-2 alone, but not observed in CD56^{bright} NK cells from any HSCT recipients with aGVHD that were assessed (Figure S1B). This was of note, as NK cells expressing TGF-β1 and exhibiting a regulatory NK cell phenotype by inhibiting T cells had been observed in other contexts.[27,30,36] We next examined whether this unique CD56^{bright} NK cells population was associated with particular immunosuppressive treatments or cancer relapse. All study participants received prophylactic post-transplant cyclophosphamide (PTCy), including those that did not develop GVHD. However, some patients that developed GVHD received additional immunosuppression for <24 h prior to sampling. When the presence of this *TGFβ1*-expressing NK cell population was compared between HSCT recipients that received PTCy alone or PTCy plus additional immunosuppression, CD56^{bright} NK cell expression of *TGFβ1* was not altered (Figures S1C and S1D; treatments detail in Table S1), indicating these additional therapies did not specifically inhibit TGF-β1-expressing NK cells. Additionally, CD56^{bright} cluster 1 proportions and *TGFB1* expression were not increased HSCT recipients that experienced cancer relapse, indicating this population is likely not correlated with inhibition of the GVL effect (Figures S1E and S1F). Collectively, the absence of this CD56^{bright} *TGFβ1*^{high} population in normal donor blood and reduction in HSCT recipients that developed GVHD suggests this population is a unique cell state in HSCT recipients protected from GVHD. We therefore next sought to identify factors that might promote NK cells to acquire this regulatory phenotype.

To identify potential signals responsible for promoting protective *TGFβ1*$^{+}$ NK cells in HSCT recipients without aGVHD, we examined expression of cytokine receptors expressed by NK cells in CD56^{bright} cluster 1, as this would indicate cytokines this population was possibly responding to (Figures 1F and S1G). Of the cytokine receptors expressed, receptors for TGFβ, (*TGFβR1*, *TGFβR2*, and *TGFβR3*) and IL-2 receptor (*IL2RA*, *IL2RB*, and *ILRG*) were highly expressed in patients without GVHD, supporting a potential role for IL-2 and TGF-β1 in driving NK cells to acquire an immunoregulatory phenotype.

IL-2 and TGF-β1 induce functional properties associated with regulatory NK cells

To explore the possibility that the combination of IL-2 and TGF-β1 confers functions in line with regulatory NK cells, we examined the combined effects of IL-2 and TGF-β1 on circulating CD56^{bright} NK cells and CD56^{dim} NK cells from healthy donors, and contrasted these effects with those of other cytokine combinations known to promote cytotoxic NK cells functions (IL-2, IL-15, and IL-18). We also assessed the impact of other cytokines that promote development of all helper ILC subsets (IL-2, IL-7, IL-23, and IL1β), cytokines that support ILC2s (IL-2, IL7, and IL-33), and cytokine receptors expressed by regulatory CD56^{+}CD3^{-} ILC population in ovarian cancer.[35] Here, CD56^{bright} CD16^{-} and CD56^{dim}CD16^{+} NK cells were isolated from healthy donor peripheral blood using flow cytometry sorting and cultured *ex vivo* with indicated cytokines to assess effects on NK cell phenotype and function (Figures 2A and 2B; Figure S2). Of all

Figure 2. CD56^{bright} NK cells expanded in IL-2 and TGF-β1 exhibit regulatory functions *in vitro*

(A) Method of NK cell isolation, PBMCs were stained with FITC conjugated antibodies for the following lineage markers: CD3, CD4, CD8α, CD14, CD15, CD19, CD20, TCRαβ, TCRδγ, CD33, CD34, CD203c, FCεr1α, CD79α, and CD138. NK were sorted as live CD56^{bright}CD16^{-} or CD56^{dim}CD16^{+}, and CCR6^{-} and CRTH2^{-} to exclude ILC2s and ILC3s.

(B) Representative gating strategy to sort CD56^{bright}CD16^{-} NK cells and CD56^{dim}CD16^{+} NK cells from healthy PBMCs.

(C) Fold expansion of NK cells after 19 days of *in vitro* culture in IL-2, IL-15, and IL-18 cytokines, or IL-2, TGF-β1, and anti-IFN-γ referred to as NK$_{conv}$ and NK$_{TGF-β}$, respectively.

(D) Representative and summary cytokine expression of CD56^{bright} NK$_{conv}$ and NK$_{TGF-β}$ at day 20 post-expansion, stimulated with phorbol 12-mystrate 13-acetate (PMA)/ionomycin for a duration of 6 h (n = 7, 3).

(E) Active TGF-β1 within supernatants of NK cells plated at 1 M/mL at D20 (n = 14, 16).

(F and G) Naive autologous CD4^{+} T cells were labeled with cell proliferation dye (CPD) for a short term 4-day culture with either NK$_{conv}$ (n = 4) or NK$_{TGF-β}$ (n = 6) with anti-CD3 and anti-CD28 antibodies. Suppression was measured by percent divided of the live CD3^{+} CD4^{+} CD56^{-} CD8^{-} in comparison to naive CD4^{+} T cells activated with anti-CD3 and anti-CD28 antibodies. Dashed line indicates 0 percent suppression.

(H) Summary of CPD^{+} HELIX-NP^{+} and Annexin-V^{+} K562 cells. Helix-NP^{+}Annexin-V^{+} indicates apoptotic cells (n = 5, 6).

(I) Expression of FOXP3 and CD25 within co-cultures with NK cells (n = 3–6).

(J) Following 20 days co-culture of CD4^{+} T cells with IL-2 and TGF-β1-treated CD56^{bright} NK cells, CD25^{+}CD127$^{low/-}$ T cells were sorted then co-cultured with CPD stained allogeneic naive T cells for 3 days (n = 3, 4). Induced Tregs (iTregs) were generated using standard induction protocols of IL-2 and TGF-β1 (n = 3, 4). Suppression as measured by percent divided of CD4^{+}CD3^{+}CPD^{+} T cells.

Asterisk indicates a significant difference, *p < 0.05; **p < 0.01; ***p < 0.001; ****p < 0.0001. Significance was determined by Kruskal-Wallis test (C–E and G), (F) Mann-Whitney U test, and (I) Signed Wilcoxon-rank test. Data are represented as mean ± SEM (D and I) or median (E, F, H, and I) are shown.

conditions tested, the combination of IL-2 and TGF-β1 could expand CD56^{bright} NK cells and had the highest upregulation NKp46 expression, which we previously observed on regulatory NK-like ILCs and linked to their immunoregulatory activity.[34] Treatment with IL-2 and TGF-β1 did not alter the percentage of CD94 co-expression with NKp46 but did decrease CD16 and degranulation marker CD107a expression in both CD56^{bright} and CD56^{dim} NK cells, in line with regulatory NK cell-like ILCs (Figure S2).

A distinguishing characteristic of regulatory NK-like ILCs has consistently been low IFN-γ and TNF-α expression, and instead the acquisition of a distinct cytokine expression profile, with differing reports of expression of IL-10, TGF-β1, IL-9, and IL-22. CD56^{bright} NK cells treated with IL-2 and TGF-β1 had a significant decrease of IFN-γ, TNF-α, and GM-CSF, and did not upregulate IL-22 or IL-9 expression, cytokines associated with ILC3s and ILC2s, respectively (Figure 2D). In addition, we did not observe expression of IL-10 (Figure 2D). However, both CD56^{bright} and CD56^{dim} NK cells treated with IL-2 and TGF-β1 (referred to hereafter as NK$_{TGF\text{-}\beta}$) acquired the ability to secrete TGF-β1 themselves, in line with the *TGFβ1*$^{+}$ NK cells associated with protection from GVHD following HSCT (Figure 2E); NK$_{TGF\text{-}\beta}$ and NK cells treated with NK cell-associated activating cytokines IL-2, IL-15, and IL-18 (referred to as NK$_{conv}$) were washed and cultured in IL-2 alone for 12–18 h, and assessed the supernatants for active TGF-β1 by cytometric bead array. Both CD56^{bright} NK$_{TGF\text{-}\beta}$ and CD56^{dim} NK$_{TGF\text{-}\beta}$ cells themselves produced active TGF-β1, with CD56^{bright} NK$_{TGF\text{-}\beta}$ having a higher average expression of 920 pg/mL ± 1.05 compared to CD56^{dim} NK$_{TGF\text{-}\beta}$ that had 530 pg/mL ± 0.66 (Figure 2E). This was of note, as NK cells that secrete TGF-β1 were reported to suppress T cell responses.[27]

Increased proportions of CD4^{+} Th1 and Th17 cells are associated with the pathophysiology of GVHD.[37] We therefore assessed whether NK$_{TGF\text{-}\beta}$ cells could inhibit naive T cell proliferation, or expression of cytokines associated with Th1 cells (IFN-γ and TNF-α) or Th17 cells (IL-17A, IL-17F, and IL-22). Expanded NK$_{conv}$ cells or NK$_{TGF\text{-}\beta}$ cells were co-cultured with cell proliferation dye labeled naive CD4^{+} T cells that were stimulated with αCD3 and αCD28 beads. After four days, the percent divided CD3^{+}CD4^{+}CD56^{-} T cells were determined based on flow cytometry analysis software (Figure 2F), and cytokine expression potential assessed by intracellular cytokine staining. After 3 days in culture with CD56^{bright} NK$_{TGF\text{-}\beta}$ cells, no change in the percent of IFN-γ, TNF-α, IL-2, or GM-CSF were observed after stimulation with PMA/ionomycin (Figure S3A). Additionally, no statistically significant impact on T cell cytokine expression was observed when CD56^{dim} NK$_{TGF\text{-}\beta}$ cells were co-cultured with naive CD4^{+} T cells compared to CD56^{dim} NK$_{conv}$ (Figure S3A). However, a consistent decrease in percent of divided T cells was observed with CD56^{bright} NK$_{TGF\text{-}\beta}$ cells (Figures 2F and 2G), indicating NK$_{TGF\text{-}\beta}$ cells could inhibit T cell proliferation.

We confirmed this decrease in T cell proliferation was not the result of CD56^{bright} NK$_{TGF\text{-}\beta}$ killing T cells, as the CD56^{bright} NK$_{TGF\text{-}\beta}$ cells did not express CD107a, a marker of recent degranulation within co-cultures and no change the number of live CD4^{+} T cells was observed (Figures S3B and S3C). Culture with CD56^{bright} NK$_{conv}$ did not limit T cell proliferation, with the exception of one experiment where a minor decrease in proliferating T cells was observed that corresponded to high CD56^{bright} NK$_{conv}$ expression of CD107a, indicating the reduction was due to NK cell-mediated T cell killing in contrast to CD56^{bright} NK$_{TGF\text{-}\beta}$ (Figure S3B). To confirm low cytotoxic potential of CD56^{bright} NK$_{TGF\text{-}\beta}$ cells and further support T cell killing did not underlie their ability to limit T cell proliferation, we assessed NK cell killing capacity toward K562 cells, an HLA class I deficient cell target commonly used to evaluate NK cell cytotoxicity. While CD56^{bright} NK$_{conv}$ cells were able to kill K562 cells, CD56^{bright} NK$_{TGF\text{-}\beta}$ cells failed to induce cell death or apoptosis, as measured by Helix-NP and Annexin-V^{+} expression, in K562 cells (Figure 2H). While CD56^{bright}NK$_{TGF\text{-}\beta}$ cells lost their cytotoxic potential, CD56^{dim} NK$_{TGF\text{-}\beta}$ cells from some donors still maintained cytotoxic potential (Figure 2H), perhaps due to CD56^{dim} being more differentiated than CD56^{bright} NK cells, and therefore less plastic.

We next explored whether NK$_{TGF\text{-}\beta}$ cells were inhibiting T cell activation, or upregulating expression of immunoregulatory molecules. We assessed T cell expression of PD-1, TIGIT, CD69, ICOS, and CD39 but did not observe altered expression of any of these markers on naive T cells (data not shown). We next asked whether NK$_{TGF\text{-}\beta}$ cells were capable of inducing T cells to develop into regulatory T cells themselves, as induced Tregs develop downstream of TGF-β1. We observed a significant fold increase of CD25^{+}FOXP3^{+}CD127^{-} T cells within CD4^{+} T cell co-cultures with CD56^{bright} NK$_{TGF\text{-}\beta}$ in comparison to stimulated T cells alone (Figure 2I), indicating CD56^{bright} NK$_{TGF\text{-}\beta}$ could promote naive CD4^{+} T cells differentiation into regulatory T cells (Tregs). To confirm these "induced" Tregs (iTregs) from CD56^{bright} NK$_{TGF\text{-}\beta}$ co-cultures were suppressive, we compared their ability to suppress T cells to FOXP3^{+} Tregs induced from naive T cells using published protocols (Cook et al., 2021, referred to as induced Treg or "iTreg").[38] CD25^{+}FOXP3^{+}CD127^{-}CD4^{+} T cells induced by NK$_{TGF\text{-}\beta}$ cells had comparable suppressive capacity to that of iTregs (Figure 2J), supporting CD56^{bright} NK$_{TGF\text{-}\beta}$ cells were capable of promoting naive T cells to differentiated into functional FOXP3^{+}Tregs.

Throughout these studies, CD56^{bright} and CD56^{dim} NK cells treated with IL-2 and TGF-β1 both expressed TGF-β1 and had similar changes in phenotype. However, CD56^{dim}-treated NK cells exhibited much greater heterogeneity in terms of cytokine profile, effects on T cells and maintained their cytotoxic potential. The difference could be due to CD56^{dim} NK cells being a more heterogeneous population, more terminally differentiated or possibly include memory-like NK cells whose phenotypes would be less plastic. Irrespective of the underlying reason, we decided to focus our studies on CD56^{bright} NK cells treated with IL-2 and TGF-β1, and further explore induced regulatory programs, as the phenotype was more pronounced and consistent between independent donors, and protective *TGFβ1*$^{+}$NK cells in HSCT recipients were CD56^{bright}.

CD56^{bright} NK$_{TGF\text{-}\beta}$ cells share a unique NK cell gene signature

In addition to NK cells, the family of innate lymphoid cells includes non-cytotoxic ILC family members comprising ~0.09% of circulating CD45^{+} cells, which are classified as group 1 ILCs

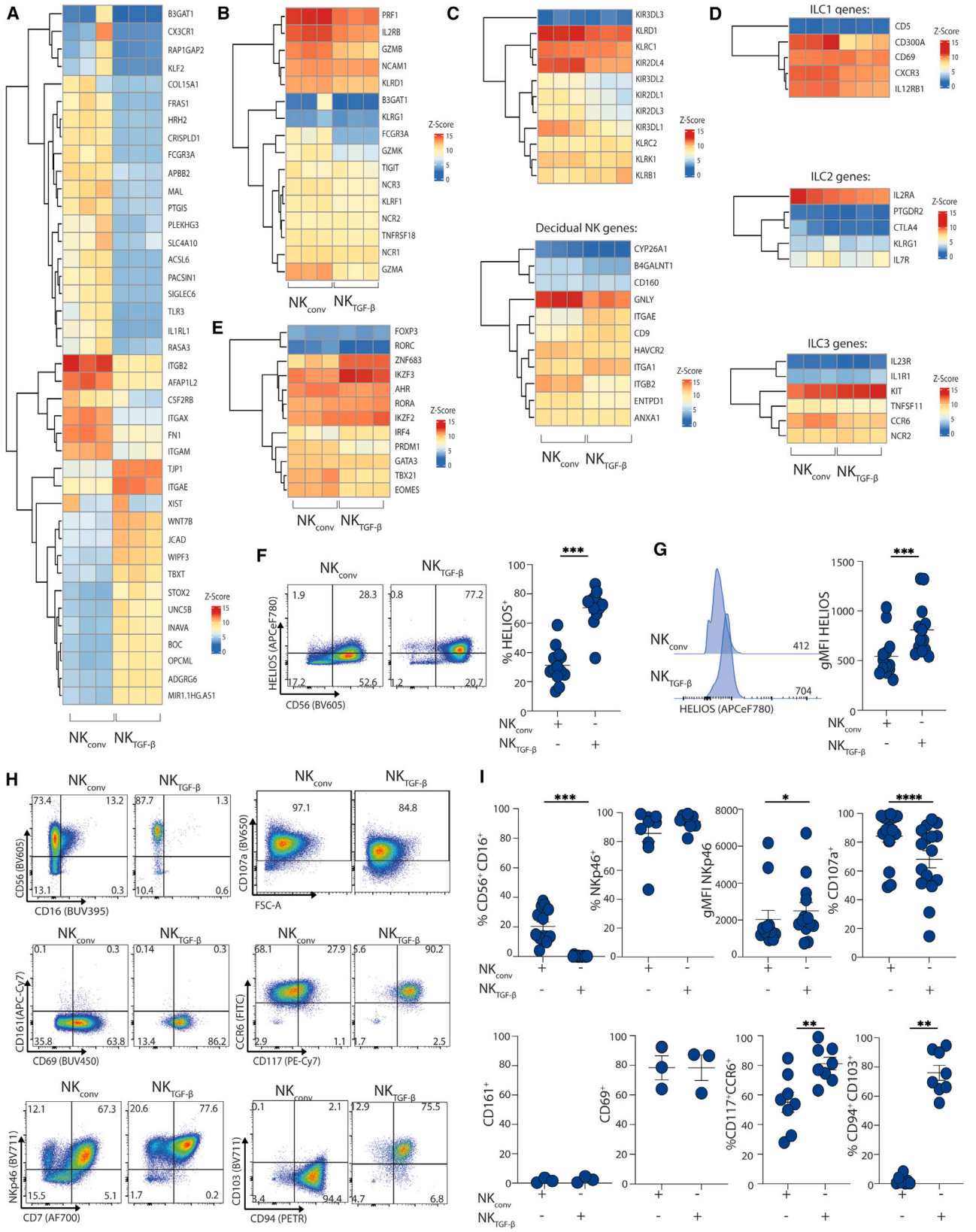

(legend on next page)

(ILC1s), group 2 ILCs (ILC2s), and group 3 ILCs (ILC3s) based on their cytokine and transcription factor expression.[39] ILC3s can express IL-22, GM-CSF, IL-17A, and IL-17F, and the transcription factor RORC2.[39] Distinguishing ILC family members sometimes presents challenges; however, ILC family members sometimes display overlapping characteristics with other ILC family members. For example, ILC3s can also express NK cell-associated molecules including CD56, NKp44, and NKp46, presenting challenges in differentiating ILC3s from NK cells.[40]

With this in mind, and to examine distinct and overlapping programs in CD56^{bright} NK$_{TGF-B}$ cells to other ILC family members, we performed bulk RNA-seq on *ex vivo* expanded CD56^{bright} NK$_{TGF-\beta}$ and CD56^{bright} NK$_{conv}$ cells, to allow unbiased transcriptome analysis, and supervised analysis of gene expression programs associated with other ILC family members. When the top differentially expressed genes were assessed, the majority of upregulated genes in CD56^{bright} NK$_{TGF-\beta}$ were genes associated with cell-cell junctions (*TJP1*, *JCAD*, *BOC*, *OPCML*, and *ADGRG6*), and transcription factors (*TBXT and STOX2*) (Figure 3A). The 27 genes downregulated are mostly attributed to surface markers (*B3GAT1*, *CX3CR1*, *FCGR3A*, *IL1RL1*, *ITGAX*, *ITGAM*, and *ITGB2*), genes involved in cytoskeleton (*FN1*, *AFAP1L2*, *COL15A1*, and *FRAS1*) and signaling pathways *(MAL*, *PLEKHG3*, and *RASA3*) (Figure 3A). Similarly, after performing gene set enrichment analysis, NK$_{TGF-\beta}$ cells downregulate networks that were highly enriched in NK$_{conv}$ cells, such as those that promote monocyte chemotaxis, neutrophil degranulation, and lymphoid killing cytotoxicity (Figure S4B). RNA-seq further confirmed CD56^{bright} NK$_{TGF-\beta}$ cells had a low cytotoxic gene signature with statically significantly lower transcriptional expression of *PRF1*, *GZMB*, *GZMK*, and *GZMA* in comparison to CD56^{bright} NK$_{conv}$ cells (Figure 3B). Whereas, for *KLRC2* encoding for NKG2C, is expressed on NK cells, had higher expression in CD56^{bright} NK$_{TGF-\beta}$ cells (0.62 log$_2$fold) but several activating and inhibitory KIRS had lower expression (*KLRD1*, *KLRC1*, *KIR3DL2*, *KIR2DL1*, *KIR2DL3*, *KIR3DL1*, and *KLRK1*), indicating a shift of NK cell function (Figure 3C). We confirmed NK cell identity by assessing molecules associated with other ILC family members. No expression of *CD5* and a decrease gene expression of other ILC1 markers including *CXCR3*, *IL12RB1*, and *CD300A* were observed (Figure 3D). Additionally, ILC2 genes including *KLRG1*, *CTLA-4*, and *PTGDR2* (CRTh2) were not statistically different between groups (Figure 3D). However, we noted *RORA*, a transcription factor associated with ILC2s, had a statistically significant fold change (0.56 log$_2$fold) in CD56^{bright} NK$_{TGF-\beta}$ cells (Figure 3E). Helper ILC3s shares several characteristics with CD56^{bright} NK$_{TGF-b}$ cells, including expression of CD56, NKp44, and NKp46, but are characterized by CD127 (*IL7R*), CD117 (*KIT*), AHR (*AHR*), and RORC2 (*RORC*) expression. We observed CD117 and CCR6 were co-expressed in CD56^{bright} NK$_{TGF-\beta}$ cells, but had significant lower expression of *RORC2* and AHR (−2.94 log$_2$fold and −0.66 log$_2$-fold, respectively), suggesting that CD56^{bright} NK$_{TGF-\beta}$ cells have similar surface marker expression but have limited overlapping transcriptional programs characteristic of ILC3s (Figure 3E).

As prior studies identified a role for TGF-β1 in promoting a decidual-like NK cell profile, we also investigated expression of decidual NK (dNK) cell-associated genes in CD56^{bright} NK cells treated with the combination of IL-2 and TGF-β1. Expression of *CD9* and *ITGA1* (CD49a), both associated with dNK cells was elevated in CD56^{bright} NK$_{TGF-\beta}$ 3.66 log$_2$fold and 2.29 log$_2$-fold higher expression, respectively[41,42](Figure 3C). Decidual NK cells have been further classified into three subsets, dNK1, dNK2, and dNK3 cells.[42] CD56^{bright} NK$_{TGF-\beta}$ had statistically lower expression of dNK1 associated genes (*ENTPD1*, *CYP26A1*, *HAVCR2*, *GNLY*, and *B4GALNT1*) and dNK2 defining gene, *ITGB2* (Figure 3C). Interestingly, there was a dichotomous gene expression of dNK3 defining genes (*ITGB2*, *CD160*, *KLRB1*, and *ITGAE)*, with a statistically significant lower expression of *ITGB2*, but higher *KLRB1* (CD161) and *ITGAE* (CD103) in CD56^{bright} NK$_{TGF-\beta}$ cells (Figure 3C). We analyzed these markers to verify protein level expression and found CD103 was highly expressed in CD56^{bright} NK$_{TGF-\beta}$ cells but there was limited expression of CD161(Figures 3H and 3I). This is in line with prior reports showing peripheral blood NK cells given TGF-β downregulate CD16 with a corresponding increase in CD103.[41] Therefore, CD103 is a distinguishing marker of IL-2 and TGF-β1-induced regulatory NK cells, a characteristic shared with both decidual NK cells and tissue resident NK cells.

We further characterized the surface marker expression to understand if there is a phenotype associated with regulatory CD56^{bright} NK$_{TGF-\beta}$ cell. Along with a decrease in CD16 expression, there was a decrease in CD7, CD107a, and GITR expression in IL-2 and TGF-β1-induced regulatory CD56^{bright} NK cells (Figures 3H and 3I; Figure S4A). *NCR1* (NKp46) and *NCR2* (NKp44), and *CD69* (CD69) were not differentially expressed transcriptionally or protein level (Figures 3H and 3I; Figure S4A). We noted, however, an increase the mean fluorescence intensity of NKp46 in CD56^{bright} NK$_{TGF-\beta}$ cells (Figures 3H and 3I), similar to our prior observation of NK cell-like regulatory ILCs from ovarian tumors.[34]

To identify transcription factors driving regulatory programs, we examined changes in expression of ILC-associated transcription factors, as well as transcription factors associated with tissue residency or regulatory T cells (Tregs). NK cell transcription factors *TBX21* (TBET) and *EOMES* (Eomes) were decreased in CD56^{bright} NK$_{TGF-\beta}$ cells, in line with prior reports of NK cells exposed to TGF-β1[43] (Figure 3E). CD56^{bright}

Figure 3. RNA-sequencing delineates transcriptional programs induced in CD56^{bright} NK cells by IL-2 and TGF-β1

(A) Heatmap representation of top 40 statistically significant differences between CD56^{bright} NK$_{conv}$ and NK$_{TGF-\beta}$ at day 20 (n = 3).

(B–D) (B) Supervised list of markers associated with NK cells and cytotoxicity, (C) KIRs, (D) ILC1, ILC2, ILC3, and decidual NK cells subsets.

(E) Heatmap representation of supervised list of transcription factors.

(F and G) (F) Percent and (G) mean fluorescence intensity by flow cytometry (n = 13).

(H and I) Representative expression (H) and (I) summary of surface markers (n = 16).

Asterisk indicates a significant difference, *p < 0.05; **p < 0.01; ***p < 0.001; ****p < 0.0001. Significance was determined by Wilcoxon test. Data are represented as mean ± SEM.

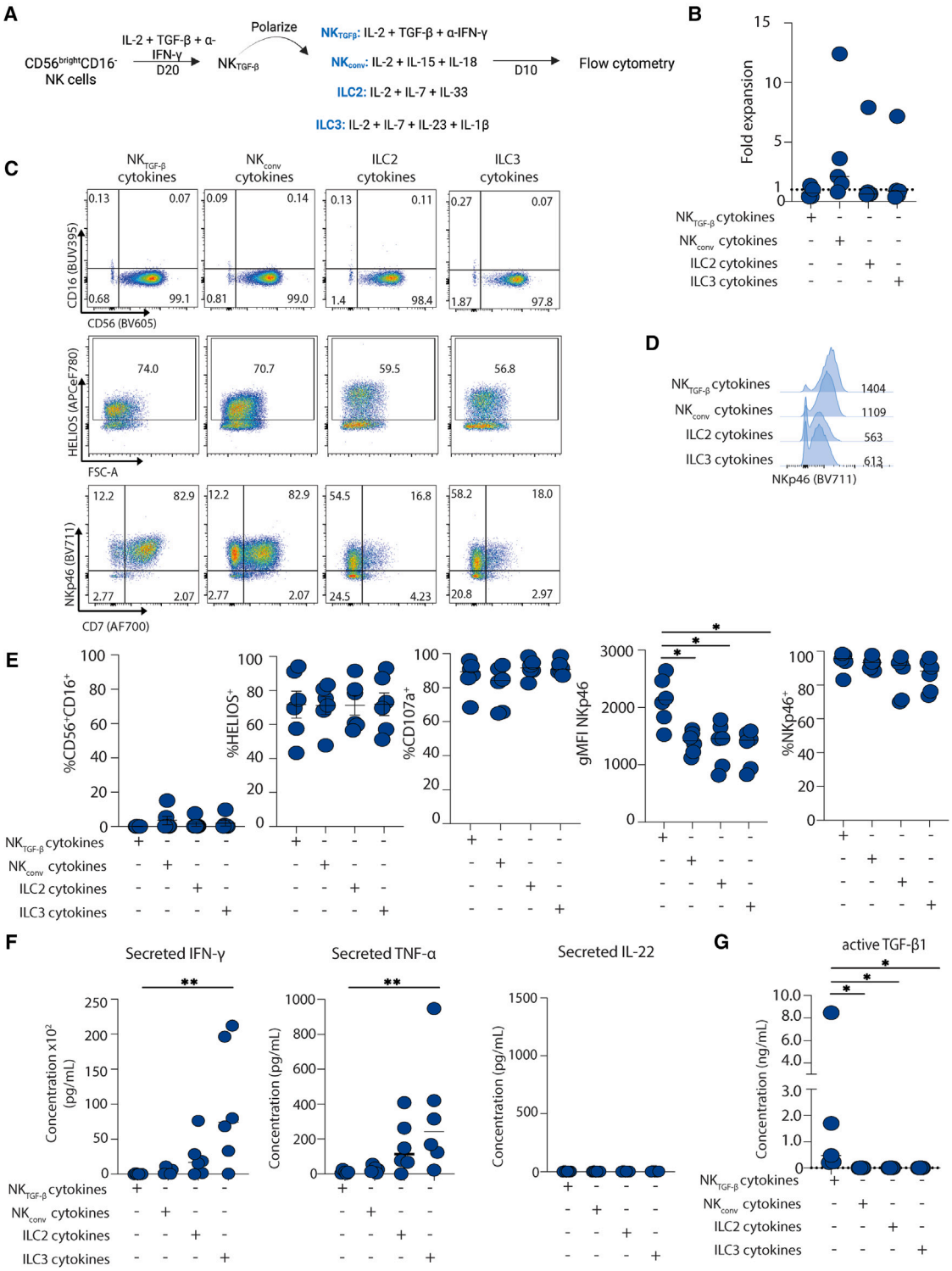

Figure 4. Investigating the plasticity of CD56^{bright} NK cells cultured in IL-2 and TGF-β1

(A) Method to investigate plasticity, 20 days post expansion of CD56^{bright} NK cells in IL-2 and TGF-β1, were then exposed to ILC2 cytokines (IL-2/7/33), ILC3 cytokines (IL-2/7/23/1β), and conventional NK cell (IL-2/15/18) cytokines, or remained in NK$_{TGF-β}$ (IL-2/TGF-β1) cytokines. *In vitro* expansion in indicated cytokines for 10 days in IL-2 (500 IU/mL), and all other cytokines used at 20 ng/mL.

(B) Fold expansion after 10 days *in vitro* (n = 5).

(C) Flow cytometry analysis surface markers and HELIOS expression of CD56^{bright} NK$_{TGF-β}$ cells cultured in indicated cytokine conditions.

(legend continued on next page)

$NK_{TGF-\beta}$ cells did not differentially express ILC2-associated *GATA3* or Treg-associated *FOXP3* (Figure 3E). However, increased expression of *ZNF683* (HOBIT), *IKZF3* (AIOLOS), and *IKZF2* (HELIOS) was observed in $CD56^{bright}$ $NK_{TGF-\beta}$ cells (Figure 3E). HELIOS expression was confirmed by flow cytometry, where both an increase in percent positive and geometric mean fluorescent intensity was observed (Figure 3F). HELIOS is a transcription factor associated with Tregs, but has also been observed in NK cells, with activity downstream of NKp46, which was notably increased by MFI with TGF-β1 treatment. Collectively, TGF-β1 and IL-2 induce a unique surface markers and transcription factor profile with overlapping characteristics to those previously reported in tissue-resident NK cells, and have decreased expression of *TBET* and *EOMES* and upregulate HELIOS, supporting altered transcriptional programs.

IL-2 and TGF-β1-induced regulatory $CD56^{bright}$ NK cells do not exhibit a stable phenotype

Having established that $CD56^{bright}$ cells in IL-2 and TGF-β1 acquire immunoregulatory functions and a distinct profile, we next examined the stability of this induced cell state. After being cultured for 21 days in IL-2 and TGF-β1, $CD56^{bright}$ $NK_{TGF-\beta}$ cells were cultured for an additional 10 days in either conventional NK cell-associated cytokines (IL-2, IL-15, and IL-18), ILC2-associated cytokines (IL-2, IL-7, and IL-33), or ILC3-associated cytokines (IL-2, IL-7, IL-23, and IL-1β) (Figure 4A). No significant change in fold expansion of $CD56^{bright}$ $NK_{TGF-\beta}$ cells was observed in these different cytokine conditions (Figure 4B), and expression of CD16, CD7, and CD107a had no statistically significantly changes in $CD56^{bright}$ $NK_{TGF-\beta}$ cells when cultured in these cytokine conditions (Figures 4C–4E). However, a decrease in the mean fluorescence intensity of NKp46 was observed, suggesting reduced levels of NKp46 expression (Figure 4D). Additionally, $CD56^{bright}$ $NK_{TGF-\beta}$ cells cultured in ILC2- or ILC3-associated cytokines regained their ability to secrete IFN-γ and TNF-α and lost the ability to secrete active TGF-β1 (Figures 4F and 4G). NK cell-associated cytokines surprisingly did not upregulate IFN-γ and TNF-α production but did abrogate the ability of $CD56^{bright}$ $NK_{TGF-\beta}$ cells to secrete active TGF-β1. Collectively these findings indicate that while IL-2 and TGF-β1 induce circulating $CD56^{bright}$ $NK_{TGF-\beta}$ cells to acquire a regulatory phenotype, this is not necessarily a stable cell state, and NK cells can still regain NK cell-associated characteristics and functions depending on microenvironment signals.

DISCUSSION

The existence of NK cells with immunosuppressive functions has been observed in a wide range of disease contexts and anatomical locations.[5,27,30] However, knowledge of factors promoting their development is relatively underexplored. In this study we identified a distinct $CD56^{bright}$ NK cell population highly expressing TGF-β1 in individuals protected from aGVHD following HSCT, which was not observed in healthy individuals and virtually absent in HSCT recipients with aGVHD. Expression of receptors for IL-2 and TGF-β1 led us to explore the impact of these cytokines on phenotypic and functional properties, and examine whether IL-2 and TGF-β1 induced regulatory in NK cells. IL-2 and TGF-β synergized to promote circulating NK cells to acquire phenotypic and functional properties in line with regulatory NK cell-like ILCs, including high expression of NKp46 and CD94, low expression of IFN-γ and TNF-α, and the ability to secrete active TGF-β1. However, this was not sufficient to induce a stable cell state, as IL-2 and TGF-β treated $CD56^{bright}$ cells lost their immunosuppressive characteristics when cultured in different cytokine conditions.

Exposure to IL-2 and TGF-β1 consistently promoted $CD56^{bright}$ NK cells to acquire suppressive functions, whereas $CD56^{dim}$ NK cells did not consistently acquire an immunosuppressive phenotype. IL-2 and TGF-β1 "induced regulatory" $CD56^{bright}$ NK cells suppressed autologous naive $CD4^+$ T cell proliferation in a cytotoxicity-independent mechanism and promoted naive T cells to develop a regulatory T cell phenotype. These induced $FOXP3^+$Tregs exhibited comparable suppressive capacity to those induced from naive $CD4^+$ T cells using established protocols. Whether this occurs in the context of HSCT, however, remains to be explored.

Importantly a distinct transcription profile was observed, with NK cells acquiring characteristics of tissue resident NK cells (expression of *ITGAE* [CD103]). The transcription factors that define NK cells, *TBX21*, and *EOMES*, were significantly reduced on $CD56^{bright}$ $NK_{TGF-\beta}$ cells, and instead *ZNF683* (HOBIT), *IKZF3* (AIOLOS), and *IKZF2* (HELIOS) were all expressed at high levels. Elevated HELIOS expression was confirmed at the protein level in $CD56^{bright}$ NK cells treated with IL-2 and TGF-β1, in addition to increased expression levels of NKp46. This was of note, as Narni-Mancinelli et al. reported in mice with a Ncr1 gene loss-of-function mutation (Noé/Noé mice), that signaling through NKp46 in Noé/Noé mice dampens NK cell responses, and $NK1.1^+CD11b^+$ NK cells in Noé/Noé mice had increased *IKZF2* transcripts compared to wild-type mice. HELIOS expression in IL-2 and TGF-β1 treated human $CD56^{bright}$ NK cells coincided with loss of both cytotoxicity and IFN-γ and TNF-α production and acquiring the ability to secrete TGF-β1. Examination of programs downstream of HELIOS in NK cells will be an interesting area to explore moving forward.

IL-2 and TGF-β1 also increased *AIOLOS*, CD103, and *HOBIT* expression that correlates with promoting a resident memory phenotype. AIOLOS is expressed by ILC1s and NK cells and when suppressed it prevented the differentiation of ILC3s toward NK cells and ILC1s.[44] In mouse, AIOLOS is constitutively expressed throughout NK cell development, and alters expression

(D) MFI of NKp46 cultured in indicated cytokines.
(E) Summary graphs of surface marker expression and HELIOS in indicated cytokine conditions (n = 5–6).
(F and G) $NK_{TGF-\beta}$ were cultured in indicated cytokines for 10 days, then counted and replated at 1 M/mL in IL-2 (500 IU/mL) overnight. Supernatants were collected and stored at −80°C to be assessed by cytokine cytometric bead array (n = 6).
Asterisk indicates a significant difference, $^*p < 0.05$; $^{**}p < 0.01$; $^{***}p < 0.001$; $^{****}p < 0.0001$. Significance was determined by repeated measures one-way ANOVA test. Data are represented as mean ± SEM.

of several hundred NK cell genes, supporting key roles in peripheral NK cell maturation.[45] CD103, also known as integrin alpha E, along with *ZNF683* that encodes for transcription factor HOBIT are widely associated with resident lymphocyte populations.[46,47] Additionally, HOBIT has been observed in ILC1s, circulating $CD56^{dim}$ NK cells and liver resident $CD56^{bright}$ NK cells, and silencing HOBIT-inhibited NK cell development from human $CD34^{+}$ cord blood progenitor cell.[48,49] The proportion of IFN-γ producing cells, however, increased with HOBIT knockdown, supporting complex functions in both NK cell development and NK cell functions.

We noted that the gene signature of IL-2 and TGF-β1 treated NK cells displayed significant overlap with the other gene signature of tissue resident NK cells defined by Dogra et al. In addition to *ITGAE* (CD103), $CD56^{bright}$ $NK_{TGF\text{-}\beta}$ upregulated *ITGA1* and downregulated markers involved in tissue egress including *S1PR1* and *KLF2*.[5] Intriguingly, $CD56^{bright}$ $NK_{TGF\text{-}\beta}$ cells downregulated *CXCR6*, a chemokine receptor associated with NK cells restricted to bone marrow, spleen, and lymph node.[5] $CXCR6^{-}$ NK cells with a tissue resident profile were reported to predominantly be found in the intestinal tract and lung.[5] As one of the primary organs impacted by GVHD is the intestinal tract, future studies should explore whether NK cells in tissues of those protected from GVHD maintain a profile consistent with these protective circulating $CD56^{bright}$ NK cells and explore if these populations can limit harmful immune responses within tissues post-HSCT.

$CD56^{bright}$ NK cells have been widely associated with protection from both acute and chronic GVHD post HSCT. We identify expression of *TGFβ1* as a defining feature of NK cells in HSCT recipients who do not develop aGVHD. NK cell with protective functions in both acute and chronic GVHD shared expression of *GZMK* expression, expression of *NCR1* (NKp46), and *CXCR3* (Figure S5).[24] Unique to our study was the determination that *TGF-β1* was expressed on regulatory NK cells associated with protection from aGVHD. This $TGFB1^{+}CD56^{bright}$ cluster 1 NK cell population also appears distinct from regulatory NK cell-like ILC populations reported in cancer, which expressed *ENTPD1* (CD73) or *CRTAM*. We noted a low CD73 expression (average of 3.7%) and no IL-10 expression, differentiating these NK cells from $CD73^{+}$ regulatory NK cells characterized in breast and sarcoma tumor patients.[27] Rather protective $CD56^{bright}$ NK cells in our study were distinguished by *TGF-β1*, *CD9*, *KLRC1* (NKG2A), and *CD69* expression. Future studies should explore the kinetics of development of these NK cells following HSCT, define their longevity within patients, and assess whether they traffic to tissues and exhibit local protective functions to prevent GVHD in different anatomical locations.

Limitations of the study

Our study utilized scRNA-seq to assess differences in NK cells between individuals who do or do not develop GVHD following HSCT. While cytokine and cytokine receptor differences were identified as a defining factor of the $CD56^{bright}$Cluster 1 that was expanded in HSCT recipients protected from GVHD, additional factors likely impact the development and function of this unique NK cell state. Further, the relatively small size of our HSCT cohort limits our ability to comment on how variables between patients impacted our data, particularly the type of cancer, type of HSCT transplant, and time from transplant. Indeed, the relatively small sample size and sampling at only one time point prevents us from determining whether the $TGFB1^{+}$ NK cells observed in patients without aGVHD have a role in directly preventing aGVHD development, or are instead part of cellular circuits that do not promote GVHD post-HSCT. However, flow cytometry analysis of active TGF-β1 expression by $CD56^{bright}$ NK cells post-HSCT in Figure S1B supports that TGF-β1-expressing $CD56^{bright}$ NK cells is correlated HSCT recipients that do not have GVHD. Our *in vitro* experiments with healthy donor blood highlight the role of the combination of IL-2 and TGF-β1 in promoting $CD56^{bright}$ NK cells to acquire at least some characteristics of these NK cells associated with protection post-HSCT. However, due to the limited availability and small number of peripheral blood mononuclear cells (PBMCs) available from samples of patients with or without GVHD post-HSCT based on study design, we could only assess TGF-β1 expression in *ex vivo* $CD56^{bright}$ NK cells, and were unable to ability perform extensive flow cytometry phenotyping and functional assays is parallel to IL-2 and TGF-β1-induced NK cells. Due to study design, we did not include analysis of when this population arises temporally, and for how long this unique cell state is observed, which would be interesting to pursue in follow up studies. We were also not powered to assess associations of sex, gender, or both on the results.

RESOURCE AVAILABILITY

Lead contact

Further information and requests for resources and reagents should be directed to the lead contact, Dr Sarah Q. Crome (sarah.crome@utoronto.ca).

Materials availability

This study did not generate new unique reagents.

Data and code availability

- scRNA-seq data can be accessed via GEO using accession code GSE255298.
- This paper does not report original code.
- Additional information needed to reanalyze the data reported in this paper and permitted by UHN REB 19–6351 is available from the lead contact upon request.

ACKNOWLEDGMENTS

First and foremost, we would like to thank the HSCT recipients at UHN who made this work possible. We would also like to thank the nurses, physicians, and surgeons at Princess Margaret Cancer Centre for efforts to obtain samples, and acknowledge technical support provided by the Princess Margaret Genomics Cent, particularly Troy Ketela and Julissa Tsao, and the Princess Margaret Cancer Centre flow cytometry core. S.Q.C. holds a Tier 2 Canada Research Chair in Tissue-Specific Immune Tolerance. This research was supported by funding from the Canadian Institutes of Health Research (169084) and the Natural Sciences and Engineering Research Council of Canada (RGPIN-2021-03672). S.Q.C. was also supported by the Medicine by Design program (Canada First Research Excellence Fund), the Ajmera Transplant Centre and Canadian Foundation for Innovation (CFI) grant 38308. Schematic figures were created with BioRender.com.

AUTHOR CONTRIBUTIONS

J.A.M. and S.Q.C. designed and implemented IL-2 and TGF-β1 studies. K.T.R., A.S.C., J.M., and S.Q.C. designed HSCT patient-based studies. D.T.B., K.T.R., and J.M.M. share co-second authorship. J.M. established the Hans Messner biobank and the infrastructure required to enable this study. A.S.C., I.N.B., T.A.M., and J.M. liaised with patient care teams to obtain human samples for study. J.A.M., K.T.R., J.M.M., S.J.C., and S.Q.C. developed ILC isolation and expansion methods. J.A.M., D.T.B., K.T.R., J.M.M., and S.J.C. performed experiments and analyzed data. K.T.R. and J.M.M. designed and implemented the bioinformatic pipeline, with advice from S.Q.C. P.S.O. advised on analysis and interpretations. S.Q.C. supervised the work. J.A.M., K.T.R., and S.Q.C. wrote the manuscript, which all authors reviewed and edited.

DECLARATION OF INTERESTS

The authors have submitted a provisional patent application# 63/353,823 with regards to effects of TGF-β1 and IL-2 on human NK cells.

STAR★METHODS

Detailed methods are provided in the online version of this paper and include the following:

- KEY RESOURCES TABLE
- EXPERIMENTAL MODEL AND STUDY PARTICPANT DETAILS
  - Human Hematopoietic stem cell transplant and healthy peripheral blood mononuclear cell samples
  - Cell lines
- METHOD DETAILS
  - Single cell RNA-sequencing
  - Natural Killer cell isolation
  - Natural Killer cell expansion
  - K562 cell killing assay
  - Naive T cell co-culture assay
  - Flow cytometry
  - Cytokine and active TGF-β1 analysis
  - RNA preparation and sequencing analysis
- QUANTIFICATION AND STATISTICAL ANALYSIS

SUPPLEMENTAL INFORMATION

Supplemental information can be found online at https://doi.org/10.1016/j.isci.2024.111416.

Received: December 21, 2023
Revised: February 7, 2024
Accepted: November 14, 2024
Published: November 18, 2024

REFERENCES

1. Langers, I., Renoux, V.M., Thiry, M., Delvenne, P., and Jacobs, N. (2012). Natural killer cells: Role in local tumor growth and metastasis. Biologics. *6*, 73–82.
2. Jegatheeswaran, S., Mathews, J.A., and Crome, S.Q. (2021). Searching for the Elusive Regulatory Innate Lymphoid Cell. J. Immunol. *207*, 1949–1957.
3. Murphy, J.M., Ngai, L., Mortha, A., and Crome, S.Q. (2022). Tissue-Dependent Adaptations and Functions of Innate Lymphoid Cells. Front. Immunol. *13*, 836999.
4. Mak, M.L., Reid, K.T., and Crome, S.Q. (2023). Protective and pathogenic functions of innate lymphoid cells in transplantation. Clin. Exp. Immunol. *213*, 23–39.
5. Dogra, P., Rancan, C., Ma, W., Toth, M., Senda, T., Carpenter, D.J., Kubota, M., Matsumoto, R., Thapa, P., Szabo, P.A., et al. (2020). Tissue Determinants of Human NK Cell Development, Function, and Residence. Cell *180*, 749–763.e13.
6. Cooper, M.A., Fehniger, T.A., and Caligiuri, M.A. (2001). The biology of human natural killer-cell subsets. Trends Immunol. *22*, 633–640.
7. Caligiuri, M.A. (2008). Human natural killer cells. Blood *112*, 461–469.
8. Lanier, L.L., Le, A.M., Civin, C.I., Loken, M.R., and Phillips, J.H. (1986). The relationship of CD16 (Leu-11) and Leu-19 (NKH-1) antigen expression on human peripheral blood NK cells and cytotoxic T lymphocytes. J. Immunol. *136*, 4480–4486.
9. Nagler, A., Lanier, L.L., Cwirla, S., and Phillips, J.H. (1989). Comparative studies of human FcRIII-positive and negative natural killer cells. J. Immunol. *143*, 3183–3191.
10. Horowitz, A., Strauss-Albee, D.M., Leipold, M., Kubo, J., Nemat-Gorgani, N., Dogan, O.C., Dekker, C.L., Mackey, S., Maecker, H., Swan, G.E., et al. (2013). Genetic and Environmental Determinants of Human NK Cell Diversity Revealed by Mass Cytometry. Sci. Transl. Med. *5*, 208ra145.
11. Romee, R., Schneider, S.E., Leong, J.W., Chase, J.M., Keppel, C.R., Sullivan, R.P., Cooper, M.A., and Fehniger, T.A. (2012). Cytokine activation induces human memory-like NK cells. Blood *120*, 4751–4760.
12. Minculescu, L., Fischer-Nielsen, A., Haastrup, E., Ryder, L.P., Andersen, N.S., Schjoedt, I., Friis, L.S., Kornblit, B.T., Petersen, S.L., Sengelov, H., and Marquart, H.V. (2020). Improved Relapse-Free Survival in Patients With High Natural Killer Cell Doses in Grafts and During Early Immune Reconstitution After Allogeneic Stem Cell Transplantation. Front. Immunol. *11*, 1068.
13. Minculescu, L., Marquart, H.V., Friis, L.S., Petersen, S.L., Schiødt, I., Ryder, L.P., Andersen, N.S., and Sengeloev, H. (2016). Early Natural Killer Cell Reconstitution Predicts Overall Survival in T Cell–Replete Allogeneic Hematopoietic Stem Cell Transplantation. Biol. Blood Marrow Transplant. *22*, 2187–2193.
14. Sheng, L., Mu, Q., Wu, X., Yang, S., Zhu, H., Wang, J., Lai, Y., Wu, H., Sun, Y., Hu, Y., et al. (2020). Cytotoxicity of Donor Natural Killer Cells to Allo-Reactive T Cells Are Related With Acute Graft-vs.-Host-Disease Following Allogeneic Stem Cell Transplantation. Front. Immunol. *11*, 1534.
15. Jagasia, M., Arora, M., Flowers, M.E.D., Chao, N.J., McCarthy, P.L., Cutler, C.S., Urbano-Ispizua, A., Pavletic, S.Z., Haagenson, M.D., Zhang, M.J., et al. (2012). Risk factors for acute GVHD and survival after hematopoietic cell transplantation. Blood *119*, 296–307.
16. Al Malki, M.M., Gendzekhadze, K., Yang, D., Mokhtari, S., Parker, P., Karanes, C., Palmer, J., Snyder, D., Forman, S.J., Nademanee, A., and Nakamura, R. (2020). Long-Term Outcome of Allogeneic Hematopoietic Stem Cell Transplantation from Unrelated Donor Using Tacrolimus/Sirolimus-based GvHD Prophylaxis: Impact of HLA Mismatch. Transplantation *104*, 1070–1080.
17. Ballen, K., Logan, B.R., Chitphakdithai, P., Kuxhausen, M., Spellman, S.R., Adams, A., Drexler, R.J., Duffy, M., Kemp, A., King, R., et al. (2020). Unlicensed umbilical cord blood units provide a safe and effective graft source for a diverse population: a study of 2456 umbilical cord blood recipients. Biol. Blood Marrow Transplant. *26*, 745–757.
18. Holtan, S.G., Yu, J., Choe, H.K., Paranagama, D., Tang, J., Naim, A., Galvin, J., and Joachim Deeg, H. (2022). Disease progression, treatments, hospitalization, and clinical outcomes in acute GVHD: a multicenter chart review. Bone Marrow Transplant. *57*, 1581–1585.
19. Ullrich, E., Salzmann-Manrique, E., Bakhtiar, S., Bremm, M., Gerstner, S., Herrmann, E., Bader, P., Hoffmann, P., Holler, E., Edinger, M., and Wolff, D. (2016). Relation between acute GVHD and NK cell subset reconstitution following allogeneic stem cell transplantation. Front. Immunol. *7*, 595.
20. Simonetta, F., Alvarez, M., and Negrin, R.S. (2017). Natural killer cells in graft-versus-host-disease after allogeneic hematopoietic cell transplantation. Front. Immunol. *8*, 465.

21. Munneke, J.M., Björklund, A.T., Mjösberg, J.M., Garming-Legert, K., Bernink, J.H., Blom, B., Huisman, C., van Oers, M.H.J., Spits, H., Malmberg, K.J., and Hazenberg, M.D. (2014). Activated innate lymphoid cells are associated with a reduced susceptibility to graft-versus-host disease. Blood *124*, 812–821.

22. Soiffer, R.J., Gonin, R., Murray, C., Robertson, M.J., Cochran, K., Chartier, S., Cameron, C., Daley, J., Levine, H., and Nadler, L.M. (1993). Prediction of graft-versus-host disease by phenotypic analysis of early immune reconstitution after CD6-depleted allogeneic bone marrow transplantation. Blood *82*, 2216–2223.

23. Ruggeri, L., Capanni, M., Urbani, E., Perruccio, K., Shlomchik, W.D., Tosti, A., Posati, S., Rogaia, D., Frassoni, F., Aversa, F., et al. (2002). Effectiveness of donor natural killer cell aloreactivity in mismatched hematopoietic transplants. Science *295*, 2097–2100.

24. Lauener, M.P., AzadPour, S., Abdossamadi, S., Parthasarathy, V., Ng, B., Ostroumov, E., Cuvelier, G.D., Levings, M.K., MacDonald, K.N., Kariminia, A., and Schultz, K.R. (2023). CD56brightCD16- natural killer cells as an important regulatory mechanism in chronic graft-versus-host disease. Haematologica *108*, 761–771.

25. Cuvelier, G.D., Kariminia, A., Nemecek, E.R., Kitko, C., Wahlstrom, J.T., Harris, A.C., Bittencourt, H., Lewis, V.A., Pulsipher, M.A., Schechter-Finkelstein, T., et al. (2020). Naïve Helper T-Cell and Regulatory T- and NK-Cell Subsets Are Associated with Pediatric Chronic Graft-Versus-Host Disease: Results of the ABLE/PBMTC 1202 Study. Blood *136*, 11–12.

26. Deniz, G., Erten, G., Kücüksezer, U.C., Kocacik, D., Karagiannidis, C., Aktas, E., Akdis, C.A., and Akdis, M. (2008). Regulatory NK Cells Suppress Antigen-Specific T Cell Responses. J. Immunol. *180*, 850–857.

27. Neo, S.Y., Yang, Y., Record, J., Ma, R., Chen, X., Chen, Z., Tobin, N.P., Blake, E., Seitz, C., Thomas, R., et al. (2020). CD73 immune checkpoint defines regulatory NK cells within the tumor microenvironment. J. Clin. Invest. *130*, 1185–1198.

28. Burrack, K.S., Huggins, M.A., Taras, E., Dougherty, P., Henzler, C.M., Yang, R., Alter, S., Jeng, E.K., Wong, H.C., Felices, M., et al. (2018). Interleukin-15 Complex Treatment Protects Mice from Cerebral Malaria by Inducing Interleukin-10-Producing Natural Killer Cells. Immunity *48*, 760–772.e4.

29. Picard, E., Godet, Y., Laheurte, C., Dosset, M., Galaine, J., Beziaud, L., Loyon, R., Boullerot, L., Lauret Marie Joseph, E., Spehner, L., et al. (2019). Circulating NKp46 + Natural Killer cells have a potential regulatory property and predict distinct survival in Non-Small Cell Lung Cancer. Oncoimmunology *8*, e1527498.

30. Ramírez-Ramírez, D., Padilla-Castañeda, S., Galán-Enríquez, C.S., Vadillo, E., Prieto-Chávez, J.L., Jiménez-Hernández, E., Vilchis-Ordóñez, A., Sandoval, A., Balandrán, J.C., Pérez-Tapia, S.M., et al. (2019). CRTAM + NK cells endowed with suppressor properties arise in leukemic bone marrow. J. Leukoc. Biol. *105*, 999–1013.

31. Thacker, G., Henry, S., Nandi, A., Debnath, R., Singh, S., Nayak, A., Susnik, B., Boone, M.M., Zhang, Q., Kesmodel, S.B., et al. (2023). Immature natural killer cells promote progression of triple-negative breast cancer. Sci. Transl. Med. *15*, eabl4414.

32. Gao, Y., Souza-Fonseca-Guimaraes, F., Bald, T., Ng, S.S., Young, A., Ngiow, S.F., Rautela, J., Straube, J., Waddell, N., Blake, S.J., et al. (2017). Tumor immunoevasion by the conversion of effector NK cells into type 1 innate lymphoid cells. Nat. Immunol. *18*, 1004–1015. https://doi.org/10.1038/ni.3800.

33. Cortez, V.S., Cervantes-Barragan, L., Robinette, M.L., Bando, J.K., Wang, Y., Geiger, T.L., Gilfillan, S., Fuchs, A., Vivier, E., Sun, J.C., et al. (2016). Transforming growth factor-β signaling guides the differentiation of innate lymphoid cells in salivary glands. Immunity *44*, 1127–1139.

34. Crome, S.Q., Nguyen, L.T., Lopez-Verges, S., Yang, S.Y.C., Martin, B., Yam, J.Y., Johnson, D.J., Nie, J., Pniak, M., Yen, P.H., et al. (2017). A distinct innate lymphoid cell population regulates tumor-associated T cells. Nat. Med. *23*, 368–375. https://doi.org/10.1038/nm.4278.

35. Hao, Y., Hao, S., Andersen-Nissen, E., Mauck, W.M., 3rd, Zheng, S., Butler, A., Lee, M.J., Wilk, A.J., Darby, C., Zager, M., et al. (2021). Integrated analysis of multimodal single-cell data. Cell *184*, 3573–3587.e29.

36. Oka, N., Markova, T., Tsuzuki, K., Li, W., El-Darawish, Y., Pencheva-Demireva, M., Yamanishi, K., Yamanishi, H., Sakagami, M., Tanaka, Y., and Okamura, H. (2020). IL-12 regulates the expansion, phenotype, and function of murine NK cells activated by IL-15 and IL-18. Cancer Immunol. Immunother. *69*, 1699–1712.

37. Yu, Y., Wang, D., Liu, C., Kaosaard, K., Semple, K., Anasetti, C., and Yu, X.Z. (2011). Prevention of GVHD while sparing GVL effect by targeting Th1 and Th17 transcription factor T-bet and RORγt in mice. Blood *118*, 5011–5020.

38. Cook, L., Reid, K.T., Häkkinen, E., de Bie, B., Tanaka, S., Smyth, D.J., White, M.P., Wong, M.Q., Huang, Q., Gillies, J.K., et al. (2021). Induction of stable human FOXP3+ Tregs by a parasite-derived TGF-β mimic. Immunol. Cell Biol. *99*, 833–847.

39. Vivier, E., Artis, D., Colonna, M., Diefenbach, A., Di Santo, J.P., Eberl, G., Koyasu, S., Locksley, R.M., McKenzie, A.N.J., Mebius, R.E., et al. (2018). Innate Lymphoid Cells: 10 Years On. Cell *174*, 1054–1066. https://doi.org/10.1016/j.cell.2018.07.017.

40. Crellin, N.K., Trifari, S., Kaplan, C.D., Cupedo, T., and Spits, H. (2010). Human NKp44+IL-22+ cells and LTi-like cells constitute a stable RORC+ lineage distinct from conventional natural killer cells. J. Exp. Med. *207*, 281–290.

41. Keskin, D.B., Allan, D.S.J., Rybalov, B., Andzelm, M.M., Stern, J.N.H., Kopcow, H.D., Koopman, L.A., and Strominger, J.L. (2007). TGFβ promotes conversion of CD16+ peripheral blood NK cells into CD16- NK cells with similarities to decidual NK cells. Proc. Natl. Acad. Sci. USA *104*, 3378–3383.

42. Vento-Tormo, R., Efremova, M., Botting, R.A., Turco, M.Y., Vento-Tormo, M., Meyer, K.B., Park, J.E., Stephenson, E., Polański, K., Goncalves, A., et al. (2018). Single-cell reconstruction of the early maternal–fetal interface in humans. Nature *563*, 347–353.

43. Harmon, C., Jameson, G., Almuaili, D., Houlihan, D.D., Hoti, E., Geoghegan, J., Robinson, M.W., and O'Farrelly, C. (2019). Liver-derived TGF-β maintains the eomeshitbetlo phenotype of liver resident natural killer cells. Front. Immunol. *10*, 1502–1509.

44. Mazzurana, L., Forkel, M., Rao, A., Van Acker, A., Kokkinou, E., Ichiya, T., Almer, S., Höög, C., Friberg, D., and Mjösberg, J. (2019). Suppression of Aiolos and Ikaros expression by lenalidomide reduces human ILC3−ILC1/NK cell transdifferentiation. Eur. J. Immunol. *49*, 1344–1355.

45. Holmes, M.L., Huntington, N.D., Thong, R.P.L., Brady, J., Hayakawa, Y., Andoniou, C.E., Fleming, P., Shi, W., Smyth, G.K., Degli-Esposti, M.A., et al. (2014). Peripheral natural killer cell maturation depends on the transcription factor Aiolos. EMBO J. *33*, 2721–2734.

46. Parga-Vidal, L., Behr, F.M., Kragten, N.A.M., Nota, B., Wesselink, T.H., Kavazović, I., Covill, L.E., Schuller, M.B.P., Bryceson, Y.T., Wensveen, F.M., et al. (2021). Hobit identifies tissue-resident memory t cell precursors that are regulated by eomes. Sci. Immunol. *6*, eabg3533.

47. Zundler, S., Becker, E., Spocinska, M., Slawik, M., Parga-Vidal, L., Stark, R., Wiendl, M., Atreya, R., Rath, T., Leppkes, M., et al. (2019). Hobit- and Blimp-1-driven CD4+ tissue-resident memory T cells control chronic intestinal inflammation. Nat. Immunol. *20*, 514.

48. Lunemann, S., Martrus, G., Goebels, H., Kautz, T., Langeneckert, A., Salzberger, W., Koch, M., J. Bunders, M., Nashan, B., van Gisbergen, K.P., and Altfeld, M. (2017). Hobit expression by a subset of human liver-resident CD56bright Natural Killer. Sci. Rep. *7*, 1–9.

49. Post, M., Cuapio, A., Osl, M., Lehmann, D., Resch, U., Davies, D.M., Bilban, M., Schlechta, B., Eppel, W., Nathwani, A., et al. (2017). The transcription factor ZNF683/HOBIT regulates human NK-cell development. Front. Immunol. *8*, 535.

50. Zheng, G.X.Y., Terry, J.M., Belgrader, P., Ryvkin, P., Bent, Z.W., Wilson, R., Ziraldo, S.B., Wheeler, T.D., McDermott, G.P., Zhu, J., et al. (2017). Massively parallel digital transcriptional profiling of single cells. Nat. Commun. *8*, 14049.

51. McGinnis, C.S., Murrow, L.M., and Gartner, Z.J. (2019). DoubletFinder: Doublet Detection in Single-Cell RNA Sequencing Data Using Artificial Nearest Neighbors. Cell Syst. *8*, 329–337.e4.

52. Young, M.D., and Behjati, S. (2020). SoupX removes ambient RNA contamination from droplet-based single-cell RNA sequencing data. GigaScience *9*, giaa151.

53. McInnes, L., Healy, J., Saul, N., and Großberger, L. (2018). UMAP: Uniform Manifold Approximation and Projection. J. Open Source Softw. *3*, 861.

54. Blighe, K., Rana, S., and Lewis, M.E.V. (2018). Publication-ready volcano plots with enhanced colouring and labeling. https://github.com/kevinblighe/EnhancedVolcano.

STAR★METHODS

KEY RESOURCES TABLE

REAGENT or RESOURCE	SOURCE	IDENTIFIER
Antibodies		
FITC anti-human CD3 (clone OKT3)	BioLegend	Cat#317306; RRID:AB_571906
FITC anti-human CD3 (clone UCHT1)	BioLegend	Cat#300440; RRID:AB_314059
FITC anti-human CD4 (clone RPAT4)	BioLegend	Cat#300538; RRID:AB_2562052
FITC anti-human CD8a (clone RPAT8)	BioLegend	Cat#301050; RRID:AB_314123
FITC anti-human CD14 (clone M5E2)	BioLegend	Cat#301804; RRID:AB_314186
FITC anti-human CD15 (clone W6D3)	BioLegend	Cat#323004; RRID:AB_756009
FITC anti-human CD19 (clone HIB19)	BioLegend	Cat#302206; RRID:AB_314236
FITC anti-human CD20 (clone 2H7)	BioLegend	Cat#302304; RRID:AB_314251
FITC anti-human TCR$\alpha\beta$ (clone IP26)	BioLegend	Cat#306706; RRID:AB_314644
FITC anti-human TCR$\gamma\delta$ (clone B1)	BioLegend	Cat#331208; RRID:AB_1575108
FITC anti-human CD33 (clone HIM3-4)	BioLegend	Cat#303304; RRID:AB_314344
FITC anti-human CD34 (clone 581)	BioLegend	Cat#343504; RRID:AB_1731923
FITC anti-human CD203c (clone NP4D6)	BioLegend	Cat#324614; RRID:AB_11218991
FITC anti-human FceR1a (clone AER37)	BioLegend	Cat#334608; RRID:AB_1227653
FITC anti-human CD79a (clone HM47)	BioLegend	Cat#333512; RRID:AB_2565983
FITC anti-human CD138 (clone MI15)	BioLegend	Cat#356508; RRID:AB_2561881
PerCPCy5.5 anti-human CD94 (clone DX22)	BioLegend	Cat#305514; RRID:AB_2565522
PerCPCy5.5 anti-human NKG2D (clone 1D11)	BioLegend	Cat#320818; RRID:AB_2562792
PE anti-human CD127 (clone HIL-7R-M21)	BD	Cat#557938; RRID:AB_2296056
PE/Dazzle594 anti-human CD16 (clone 3G8)	BioLegend	Cat#302054; RRID:AB_2563638
PE-Cyanine7 anti-human CD117 (clone 104D2)	eBioscience	Cat#25-1178-42; RRID:AB_10718535
APC anti-human CD196 (clone G034e3)	BioLegend	Cat#353416; RRID:AB_10945155
APC/Cyanine7 anti-human CD45 (clone HI30)	BioLegend	Cat#304014; RRID:AB_314402
Brilliant Violet 421 anti-human CD294 (clone BM16)	BioLegend	Cat#350112; RRID:AB_2562468
Brilliant Violet 510 mouse anti-human CD336 (clone p44-8)	BD	Cat#744300; RRID:AB_2742130
Brilliant Violet 605 anti-human CD56 (clone HCD56)	BioLegend	Cat#318334; RRID:AB_2561912
Alexa Fluor 488 anti-human GITR (clone 108-17)	BioLegend	Cat#371210; RRID:AB_2650623
PerCPCy5.5 anti-human CRTAM (clone Cr24.1)	BioLegend	Cat#339112; RRID:AB_2783221
PE anti-human NKp44 (clone P44-8)	BioLegend	Cat#325108; RRID:AB_756099
PE-Dazzle594 anti-human CD294 (clone BM16)	BioLegend	Cat#350126; RRID:AB_2572052
Alexa Fluor 700 anti-human CD7 (clone CD7-6B7)	BioLegend	Cat#343126; RRID:AB_2800913
BV650 anti-human CD107a (clone H4A3)	BioLegend	Cat#328638; RRID:AB_2565838
Brilliant Violet 711 anti-human NKp46 (clone 9E2)	BioLegend	Cat#331936; RRID:AB_2650940

(*Continued on next page*)

Continued

REAGENT or RESOURCE	SOURCE	IDENTIFIER
Brilliant Violent 786 anti-human LAG3	BioLegend	Cat#369322; RRID:AB_2716127
BUV395 anti-human CD16 (clone 3G8)	BD Biosciences	Cat#563785; RRID:AB_2744293
BUV737 anti-human ICOS (clone dx29)	BD Biosciences	Cat#564778; RRID:AB_2738947
APCeF780 anti-human HELIOS (clone 22F6)	Invitrogen	Cat#47-9883-42; RRID:AB_2573998
FITC anti-human CCR6 (clone G034E3)	BioLegend	Cat#353412; RRID:AB_10916387
PerCPeF710 anti-human CD39 (clone eBioA1)	eBioscience	Cat#46-0399-42; RRID:AB_10597271
PE anti-human NKp44 (clone P44-8)	BioLegend	Cat#325108; RRID:AB_756100
PE-Dazzle594 anti-human CD94 (clone DX22)	BioLegend	Cat#305520; RRID:AB_2734277
Brilliant Violet 510 anti-human CD5 (clone L1F12)	BioLegend	Cat#364018; RRID:AB_2565728
Brilliant Violet 711 anti-human CD103 (clone Ber-ACT8)	BioLegend	Cat#350222; RRID:AB_2629651
Brilliant Violet 786 anti-human HLA-DR (clone L243)	BioLegend	Cat#307642; RRID:AB_2563461
BUV737 anti-human CD73 (clone AD2)	BD Biosciences	Cat#565395; RRID:AB_2739217
APC anti-human CD25 (clone BC96)	eBioscience	Cat#17-0259-42; RRID:AB_1582219
Brilliant Violet 605 anti-human CD4 (clone RPA-T4)	BioLegend	Cat#300556; RRID:AB_2564391
Brilliant Violet 785 anti-human PD-1 (clone EH12.2H7)	BioLegend	Cat#329930; RRID:AB_11218984
BUV395 anti-human CD3 (clone UCHT1)	BD Biosciences	Cat#563546; RRID:AB_2744387
BUV450 anti-human CD69 (clone FN50)	BD Biosciences	Cat#750214; RRID:AB_2874415
BUV737 anti-human CD16 (clone 3G8)	BD Biosciences	Cat#564434; RRID:AB_2744295
Brilliant Violet 510 anti-human CD8 (clone RPA-T8)	BioLegend	Cat#301048; RRID:AB_2561942
PECF594 anti-human FOXP3 (clone 236A/E7)	BD Biosciences	Cat#563955; RRID:AB_2738507
BV650 anti-human IL-2 (clone 5344.111)	BD Biosciences	Cat#563467; RRID:AB_2738224
FITC anti-human CCR6 (clone G034E3)	BioLegend	Cat#353412; RRID:AB_10916387
APC-Cy7 anti-human CD56 (clone HCD56)	BioLegend	Cat#318332; RRID:AB_10896424
BV711 anti-human GARP (clone 7B11)	BD Biosciences	Cat#563958; RRID:AB_2738510
BV786 anti-human PD-1 (clone EH12.2H7)	BioLegend	Cat#329930; RRID:AB_2563443
PerCPCy5.5 anti-human CD8 (clone RPA-T8)	Invitrogen	Cat#45-0088-41; RRID:AB_1582256
Biological samples		
Healthy adult peripheral blood	Canadian Blood Services	Study: 2020.047
Human HSCT peripheral blood	UHN Messner Allogeneic Transplant Program Biobank	UHN REB 19-6351
Chemicals, peptides, and recombinant proteins		
Cell proliferation dye eF450	Invitrogen	65-0842-85
Fixable Viability Dye eF450	eBioscience	65-0863-18
Fixable Viability Dye eF506	eBioscience	65-0866-18
Fixable Viability Stain 700	BD	Cat#564997; RRID:AB_2869637
Recombinant Human TGF-beta 1 (Human Cell-expressed) Protein	R&D	7754-BH-005/CF
Human IFN-gamma Antibody	R&D	MAB285-SP
rh IL-15 carrier-free	BioLegend	570306

(*Continued on next page*)

Continued

REAGENT or RESOURCE	SOURCE	IDENTIFIER
rh IL-18 carrier-free	BioLegend	592106
TheraPEAK X-VIVO-15 Serum-free Hematopoietic Cell Medium	Lonza	BEBP04-744Q
Proleukin (IL-2)	STERIMAX INC	DIN:02130181
Human TruStain FcX™	BioLegend	422302
NK MACS Medium	Miltenyi Biotec	130-114-429
rh IL-33 Protein, CF	Biolegend	581806
rh IL-23 Protein, CF	Biolegend	574106
rh IL-1b protein, CF	Biolegend	579406
rh IL-7 protein, CF	Biolegend	581908
Critical commercial assays		
EasySep FITC Positive Selection Kit II	STEMCELL	17682
Human free active total tgfbeta 1 assay	Biolegend	740450
LEGENDplex™ HU Th Cytokine Panel (12-plex) w/VbP V02	Biolegend	741028
Deposited data		
Single cell RNA-seq data	https://www.ncbi.nlm.nih.gov/geo/query/acc.cgi	Dataset can be accessed using GEO accession code GSE255298
Experimental models: Cell lines		
Human K562 cells	ATCC	CCL-243
Software and algorithms		
PRISM	GraphPad Software	Version 6
FlowJo	Flowjo	Version 10.5.3
GSEA	www.gsea-msigdb.org	4.0.5
R	The R project for Statistical Computing	4.1.0
Seurat pipeline	Seurat package in R	4.0.6
UMAP	UMAP package in R	0.2.7.0
Cytoscape	Institute for Systems Biology. (2019)	https://www.cytoscape.org
Other		
Chromium Single-Cell Platform	10× Genomics Chromium	N/A
Human reference genome NCBI build 38, GRCh38	Genome Reference Consortium	https://www.ncbi.nlm.nih.gov/grc/human

EXPERIMENTAL MODEL AND STUDY PARTICPANT DETAILS

Human Hematopoietic stem cell transplant and healthy peripheral blood mononuclear cell samples

Study protocols were approved by the Research Ethics Board of the University Health Network in accordance with the Helsinki Declaration and good clinical practice guidelines (UHN REB 19–6351). All patients provided written, informed consent for collection of samples. Fresh peripheral blood for this study was collected in EDTA blood collection tubes (BD Biosciences). HSCT recipient PBMCs were obtained from the Messner Allogeneic Transplant Program Biobank, the sample size was 13. PBMCs from HSCT recipients that developed grade 3–4 GVHD were collected at time of diagnosis. PBMCs from HSCT recipients that did not develop GVHD were collected at comparable timepoints, and age and sex-matched where possible. Patient characteristics are listed in Table S1. Here, Biological sex was tracked and reported, however this study was not powered to assess associations of sex, gender, or both on the results.

Samples were prepared according to 10× Genomics Single Cell 5′ v2 Reagent kit user guide. For studies using healthy donor PBMCs, samples were collected from healthy patients through Canadian Blood Services Blood4Research Program (approved study 2020.047). All participants provided written informed consent per the netCAD Blood4Research Consent Form. Healthy donor blood was also collected according to an approved study per the Review Ethics Board policies (CAPCR ID 17–6229). The biological sex and age of patients are reported in Table S2.

Cell lines

The K562 cell line is a human lymphoblast cells isolated from the bone marrow of a 53-year-old chronic myelogenous leukemia patient and was purchased directly from ATCC. They were cultured in RPMI 1640 (Gibco) complete medium containing 10% FBS (Cytiva) and 1% Penicillin-Streptomycin (Gibco) in 5% CO_2 at 37°C. Cells were maintained at a concentration of $1 \times 10^5 - 1 \times 10^6$ viable cells/mL and were tested to ensure no mycoplasma contamination.

METHOD DETAILS

Single cell RNA-sequencing

For single-cell RNAseq experiments, isolated patient PBMCs were resuspended in 1xPBS with 0.04% BSA (Millipore Sigma) and prepared according to 10× Genomics Single Cell 5′ v2 platform in accordance with manufacturers instructions. 12,000 cells were targeted for capture from each sample, sequenced to a depth of 40,000 reads. Expression matrices and alignment to the reference human genome (GRCh38/hg38) was done using CellRanger v6.1.2.[50] Single cells were filtered to exclude cells that expressed >10% mitochondrial genes, <1000 total transcripts and <200 unique genes. Data were log normalized, principal component analysis was preformed and cells were clustered with the Louvain algorithm using FindNeighbors and FindClusters in Seurat using the top 20 principal components.[35] Doublets were excluded using the DoubleFinder package.[51] Free mRNA contamination in each droplet was estimated and removed using the SoupX package.[52] Clusters were visualized using the Uniform Manifold Approximation and Projection(UMAP).[53] NK cell clusters were subsetted based on expression of *NCAM1* and *FCGR3A* without expression of T cell markers *CD3E, CD8A* and *CD4* as well as other lineage markers. Differential expression of markers in each cluster was done using FindMarkers in Seurat and was visualized using EnhancedVolcano.[54]

Natural Killer cell isolation

PBMCs were isolated from whole blood from both male and female normal donors. Sex of normal blood donors was not available prior to receiving blood, therefore we could not include sex as a variable for this study. However, in all experiments, NK cells from both male and female donors were included, with no significant differences observed with our sample size.

Whole blood was diluting 1:1 with FACS buffer (1× PBS +2%FCS) and layered using Lymphoprep. Cells were washed in FACS, and platelets were removed by centrifugation for 10 min three times. Red blood cells were lysed with ACK Lysing Buffer (Gibco). PBMCs were stained with FITC conjugated antibodies for the following lineage markers: CD3 (OKT3), CD3 (UCHT1), CD4 (RPAT4), CD8α (RPAT8), CD14 (M5E2), CD15 (W6D3), CD19 (HIB19), CD20 (2H7), TCRαβ (IP26), TCRδγ (B1), CD33 (HIM3-4), CD34 (581), CD203c (NP4D6), FCεr1α (AER37), CD79α (HM47) and CD138 (MI15). Cells are washed in FACS buffer, resuspended in EasySep Buffer (StemCell Technologies) and enriched using the EasySep FITC Positive Selection Kit II (StemCell Technologies), as per manufacturer instructions. Enriched cells were stained with a cocktail containing CD94 (PerCPCy5.5, DX22), NKG2D (PerCPCy5.5, 1D11), CD127 (PE, HIL-7R-M21), CD16 (PE-Dazzle594, 3G8), CD117 (PE-Cy7, 1D11), CCR6 (APC, G034e3), FVS700, CD45 (APC-Cy7, HI30), CRTh2 (BV421, BM16) and CD56 (BV605, HCD56). NK were sorted as live $CD45^+Lineage^-CD56^{bright}CD16^-CCR6^-CRTH2^-$ or $CD45^+CD56^{dim}CD16^+CCR6^-CRTH2^-$ using a FACSAria Fusion (BD Biosciences).

Natural Killer cell expansion

NK cells were cultured in 500IU/mL of IL-2 (SteriMax), 20 ng/mL of IL-15 (BioLegend), 20 ng/mL of IL-18 (BioLegend) in complete MACS NK Miltenyi Medium (5% human serum, 1% supplement, 1% penicillin/streptomycin) are identified throughout as NK_{conv} for conventional NK cells. NK cells cultured in 500 IU/mL of IL-2 (SteriMax), 20 ng/mL of TGF-β1 (R&D), and 10 ng/mL of α-IFN-γ (R&D) in complete XVIVO 15 medium (supplemented with 5% human serum, 1% glutamax, 1% penicillin/streptomycin) are identified as NK_{TGFB}. Media was replenished every 2–3 days with fresh cytokines.

K562 cell killing assay

Expanded NK cells were co-cultured with cell proliferation dye labeled K562 cells at an effector-to-target ratio of 1:1 for 12 h in complete RPMI 1640 medium (10% fetal bovine serum, 1% penicillin/streptomycin, 1% glutamax) supplemented with IL-2 (100 IU/mL) in 5% CO_2 at 37°C. After 12 h, cells were harvested, stained with surface antibodies, followed by staining with Annexin-V PerCPCy5.5 and Helix-NP FITC (20nM). Samples were assessed immediately using a BD Fortessa cytometer.

Naive T cell co-culture assay

After 21 days in culture, NK cells were counted and co-cultured with autologous naive $CD4^+$ T cells. Naive T cells were isolated from frozen PBMCs using STEMCELL Naive $CD4^+$ T cell isolation kit. Following isolation, the cells were labeled with cell proliferation dye eF450 per the manufacturer's instructions. T cells were co-cultured with NK cells at a 1:1 ratio for a duration of 4 days with anti-CD3 and anti-CD28 Dynabeads (ratio of 1:8) in the absence of exogenous cytokines. Percent suppression was measured by percent divided live $CD3^+$ $CD4^+$ $CD56^-$ $CD8^-$ that were co-cultured with NK cells divided by naive $CD4^+$ T cells activated with anti-CD3 and anti-CD28 antibodies (%suppression = 100 – [%T cells of $NK_{TGF\text{-}\beta1}$/%T cells in beads alone]*100).

Flow cytometry

Following 15 min incubation with human TruStain FcX (BioLegend), staining was performed in 1× PBS supplemented with 2% fetal calf serum (FACS buffer) at 4°C. Followed by surface marker staining for 30 min at 4°C. For intracellular staining, cells were washed with FACS, fixed using the FOXP3/Transcription Factor Staining set (eBioscience) for 30 min at room temperature and permeabilized for 15 min, and then incubated with intracellular antibodies found in at room temperature for 30min. Samples were washed and re-suspended in FACS buffer and then were assessed on an LSR Fortessa (BD Biosciences). The data were analyzed using FlowJo version 10 software.

Cytokine and active TGF-β1 analysis

For secreted cytokine analysis, following expansion cells were washed three times in media without cytokines and plated in a 96-well round bottom plate at the same concentration in complete media with 500IU/mL of IL-2 alone, including a well with complete media alone as a control. Supernatants were collected after overnight incubation and were frozen at −80°C. Analytes were thawed and measured using the 12-plex LegendPlex Human Th Cytokine Panel (BioLegend) or Human active TGF-β1assay (BioLegend) as per manufacturer's instructions.

RNA preparation and sequencing analysis

NK cells were expanded as described above (and denoted as NK_{conv} or $NK_{TGF\text{-}b}$ depending on if cultured conditions) for 20 days. RNA was extracted from 100,000 cells from 3 independent donors using RNeasy Plus MiniKit (Cat74134) kit and stored in RLT solution at −80°C. RNA samples were quantified by qubit RNA kit (Life Technologies) and quality assessed by Agilent Bioananlyzer. All samples have RIN >9.6. Libraries were prepared with 15ng of total RNA using Stranded Total RNA prep with Ribo-Zero Plus kit (Illumina) with 13 cycles of amplification used. Final cDNA libraries were size validated using Agilent Bioanalyzer or Tapestation and concentration validated by qPCR (Kapa Biosystems/Roche). All libraries were normalized and pooled together, denatured with 0.2N NaOH and diluted to a final concentration of 250 p.m. Pooled libraries were loaded onto an Illumina Novaseq V1.5 cartridge for cluster generation and sequencing on an Illumina Novaseq 6000 instrument (Illumina) Paired-end 101 bp protocol to achieve ∼60 million reads per sample. Output FASTQ files were assessed for quality using the MultiQC package. Sequencing data were aligned to the GRCh38 genome (version refdata-gex-GRCh38-2020-A, 10× Genomics) using STAR aligner version 2.7.9. Feature counts were generated using the featureCount utility in the subread package, discarding multi-mapping reads. Differential expression analysis of $CD56^{bright}$ NK cells between NK_{conv} and $NK_{TGF\text{-}b}$ conditions, controlled for donor, was conducted using the DESeq2 package, and significance was calculated using the Benjamini-Hochberg adjusted *p*-value less than 1×10^{-10}. A ranked gene list for the comparison was generated using log2 fold changes and *p* values for gene set enrichment analysis using GSEA.

QUANTIFICATION AND STATISTICAL ANALYSIS

Statistical significance was determined by Kruskal-Wallis test, one way ANOVA, or Wilcoxon test and indicated in the figure legend. The number of replicates is represented by *n* and is indicated in each figure legend. $^{*}p < 0.05$; $^{**}p < 0.01$; $^{***}p < 0.001$; $^{****}p < 0.0001$; *ns*, not significant unless otherwise stated in figure legend. Data are represented as mean ± SEM unless otherwise stated. Data analysis was preformed using GraphPad Prism v9 and RStudio v4.2.3.